

Magnetisation Transfer (MT) and Chemical Exchange Saturation Transfer (CEST)



Nottingham, UK
October 15-17th

www.nottingham.ac.uk/go/3rdrenalmri

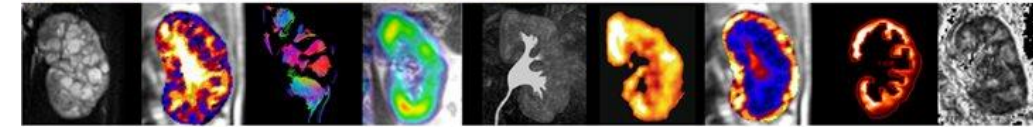
Co-organised by

UKRIN
UK Renal Imaging Network

parenchima
ESCS

cost
EUROPEAN COOPERATION
IN SCIENCE & TECHNOLOGY

Funded by the Horizon 2020 Framework Programme
of the European Union



Dario Longo, PhD
Senior Researcher
Institute of Biostructures and Bioimaging (IBB)
National Research Council of Italy (CNR)
Torino, Italy

dariolivio.longo@cnr.it

dario.longo@unito.it

www.cim.unito.it/PI/Longo/home.php



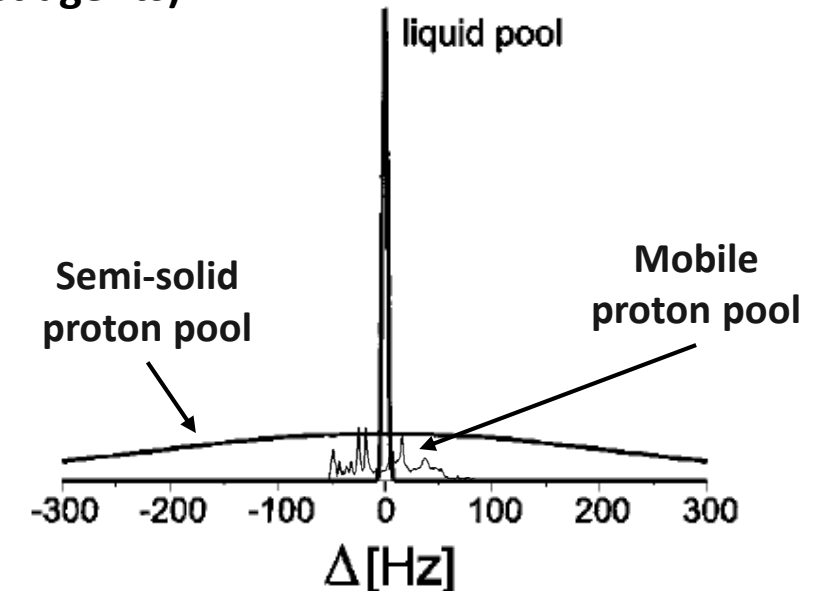
National Research Council of Italy

MAGNETIZATION TRANSFER: THEORY

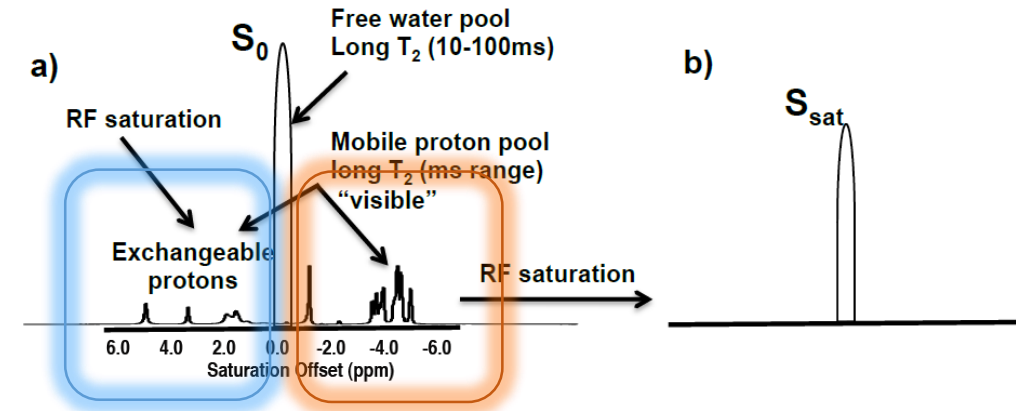
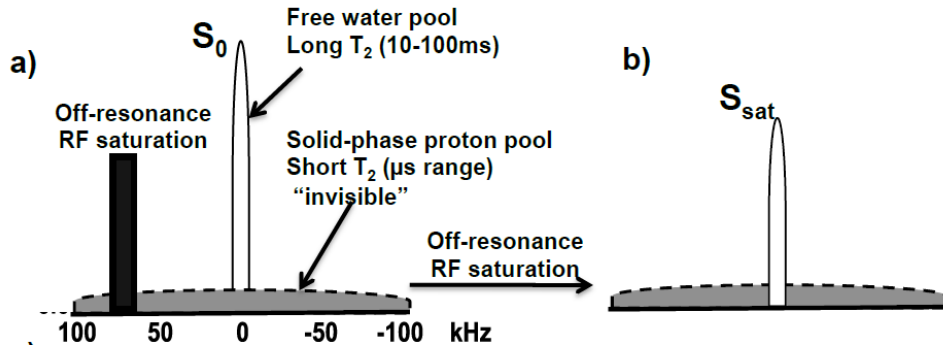
In NMR, MT (magnetization transfer) is a general term that describes the process of magnetization transfer from one spin population to another

- ❑ In MRI, MTC (**Magnetization Transfer Contrast**) denotes saturation transfer contrast originating from semi-solid macromolecules (large protein, collagen, myelin) or bound water protons with broad lineshapes (short T_2 10-100 μ s)
- ❑ In MRI, CEST (**Chemical Exchange Saturation Transfer**) denotes saturation transfer by chemical exchange originating from mobile proteins (long $T_2 > 10$ ms) and metabolites (or exogeneous contrast agents)

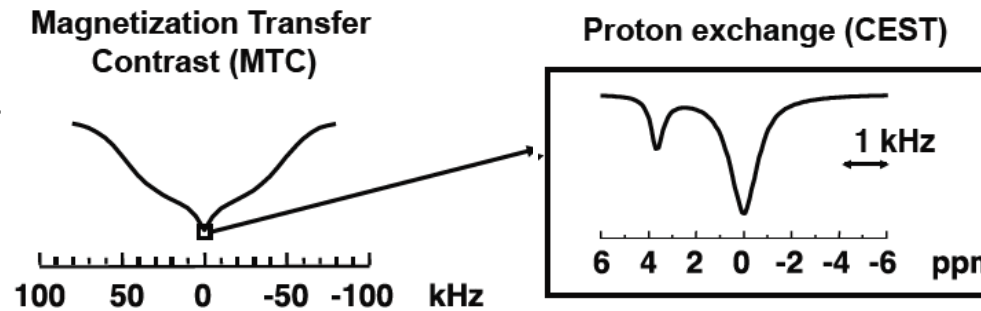
- Selective magnetic labeling of a proton pool that is stored as a change in longitudinal magnetization
- Transfer of this label to a water proton pool
- Accumulation of the label for the purpose of water signal reduction



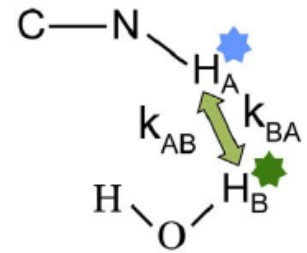
MTC AND CEST



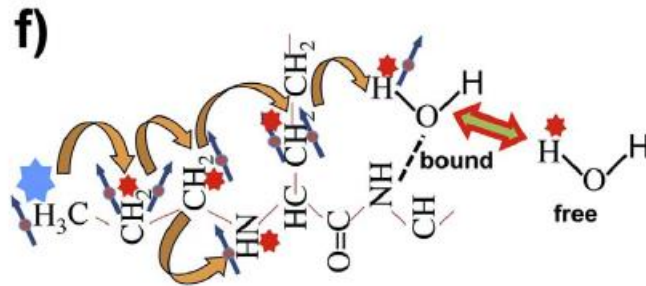
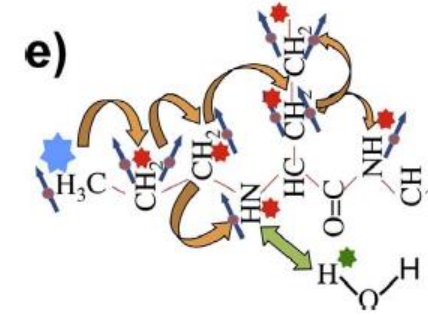
- Labelling proton pools of the semisolid macromolecular component (spin-diffusion or cross-relaxation) followed by transfer to solvent water protons by means of bound water (dipolar coupling or chemical exchange)



- Labelling of mobile protons downfield from water (chemical exchange)



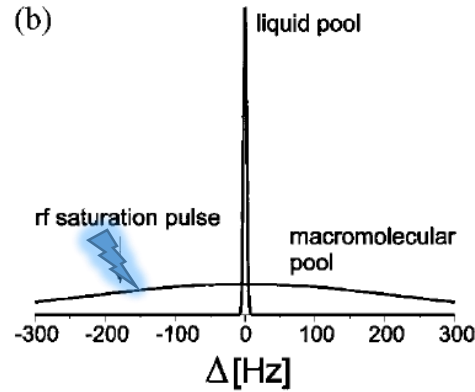
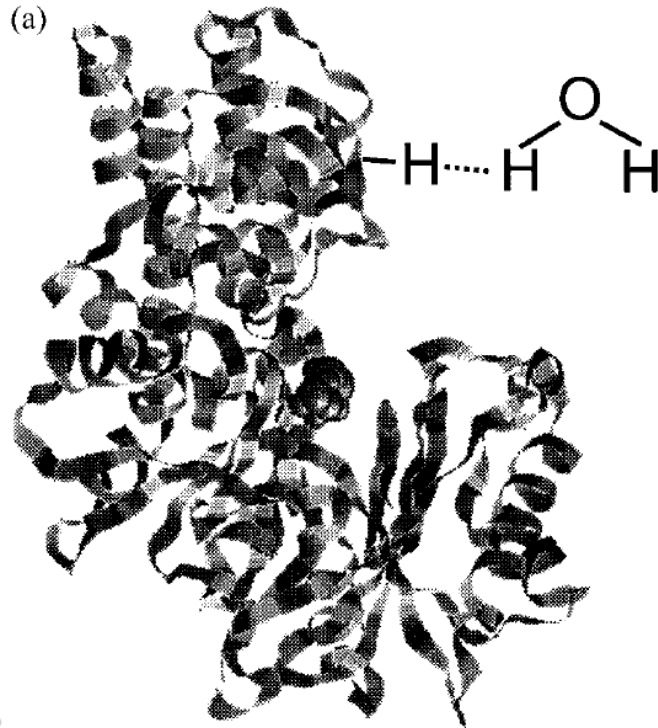
- Labelling of aliphatic proton in mobile proteins upfield from water (relayed NOE)



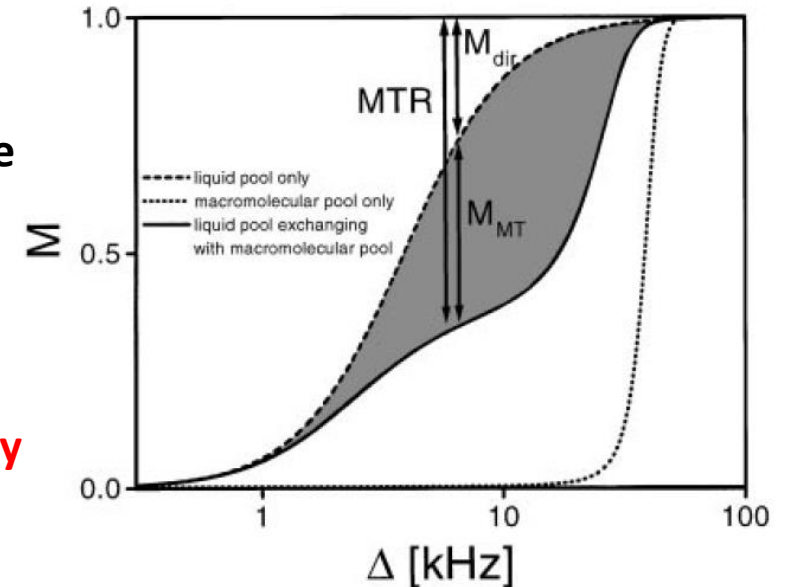
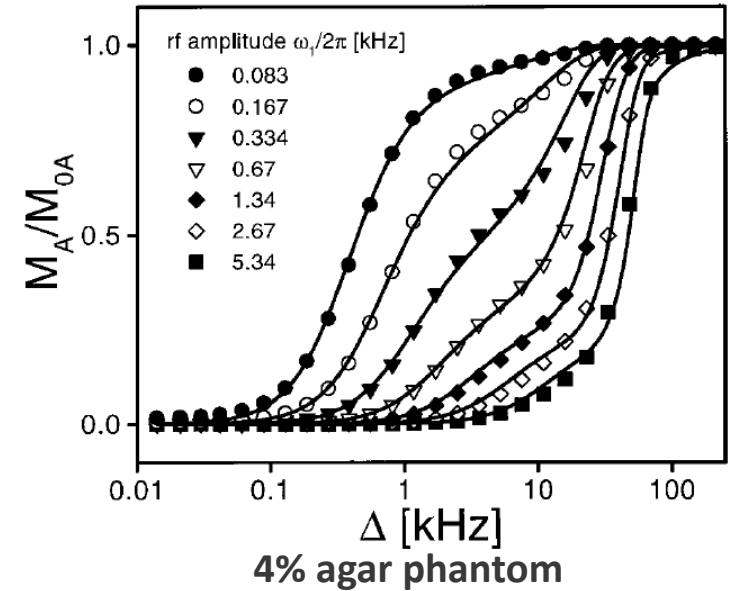
S. D. Wolff and R. S. Balaban, Magnetization transfer contrast (MTC) and tissue water proton relaxation in vivo. *Magn Reson Med*, 1989, 10, 135-144

Forsen, S., Hoffman, R.A., 1963. Study of moderately rapid chemical exchange reactions by means of nuclear magnetic double resonance. *J. Chem. Phys.* 39, 2892–2901.
 S. D. Wolff and R. S. Balaban, NMR Imaging of Labile Proton Exchange. *J. Magn. Reson.*, 1990, 86, 164-169

MAGNETIZATION TRANSFER CONTRAST



$$\text{MTR} = 1 - S_{\text{sat}}/S_0$$



Applications:

- magnetic resonance angiography (MRA) to enhance signal contrast between the blood and other tissue
- Characterization of white matter disease in the brain, principally demyelination disease (multiple sclerosis) or for assessing knee cartilage

Limitations:

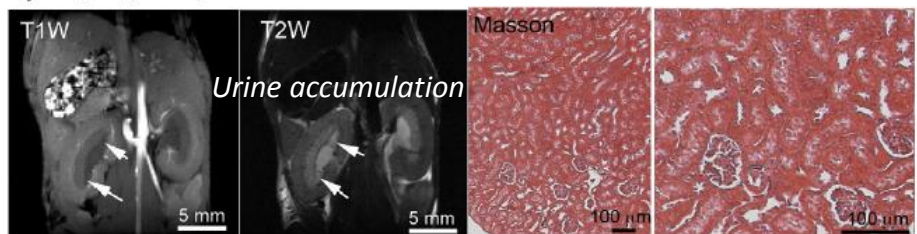
- sensitivity, specificity, and reproducibility of MTR measures can be influenced by various experimental parameters and field strength
- MTR measures tend to reflect a complex combination of sequence details and relaxation parameters

Longitudinal assessment of mouse renal injury using high-resolution anatomic and magnetization transfer MR imaging[☆]

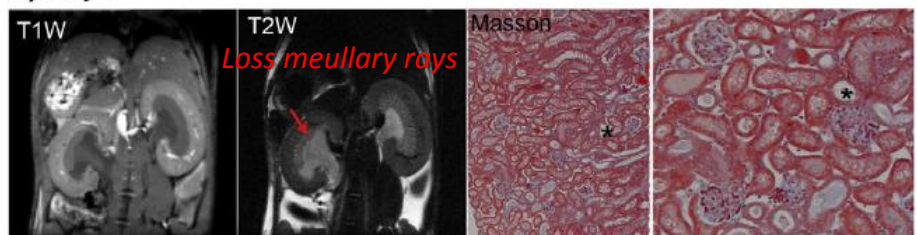
Feng Wang^{a,b}, Rosie Jiang^e, Keiko Takahashi^e, John Gore^{a,b,c,d}, Raymond C. Harris^e, Takamune Takahashi^{d,e,*}, C. Chad Quarles^{a,b,c,d,**}

- Obstructive nephropathy is a primary source of renal impairment in infants and children
- The Unilateral Ureteral Obstruction (UVO) model in mice induces serial changes in renal structure and recapitulates key features of tubular damage, apoptosis, and renal fibrosis
- **The decreased MTR values suggest reduced macromolecular content, which could be related to apoptosis, tubular atrophy and urine retention**

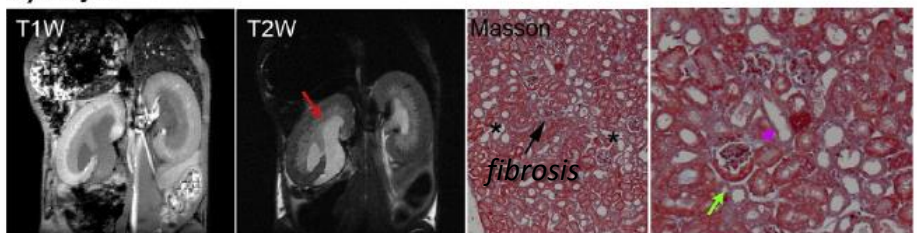
a) Day 0 (3 hrs)



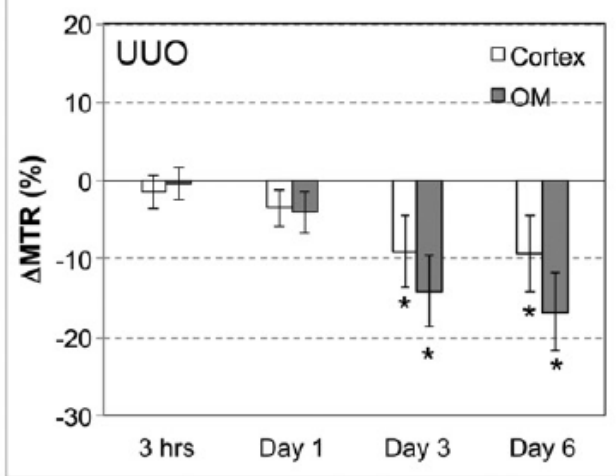
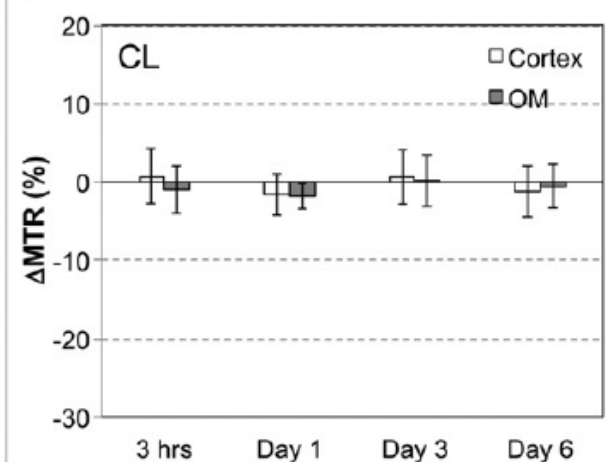
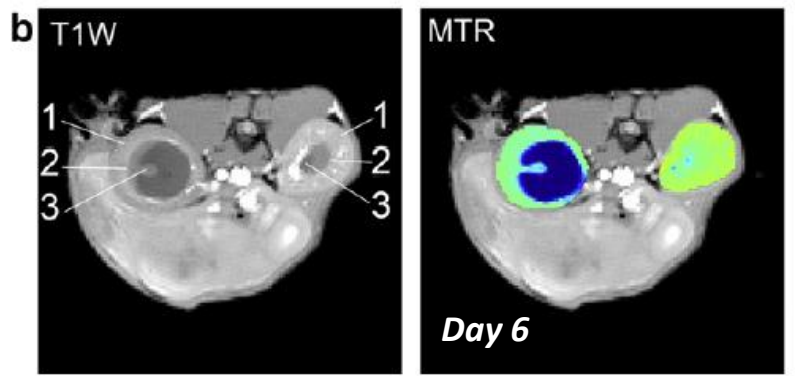
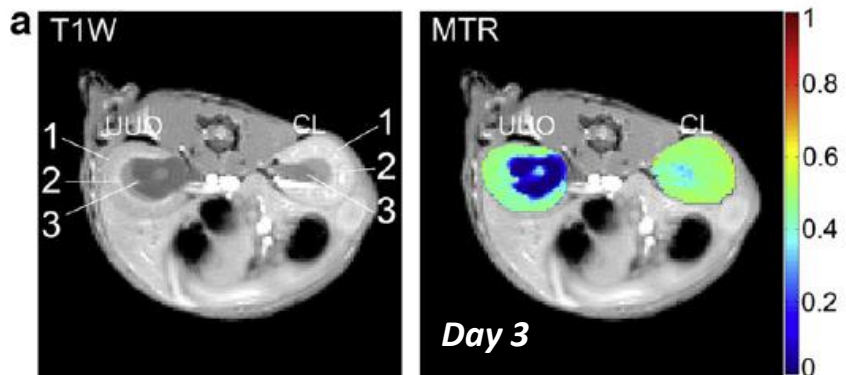
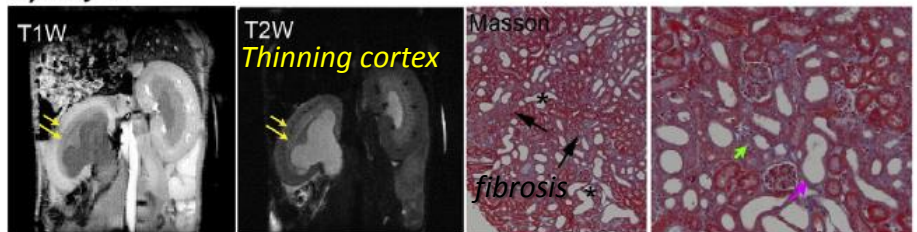
b) Day 1



c) Day 2



d) Day 6



7T, RF @20 ppm, 820° x 12ms



Italian National Research Council

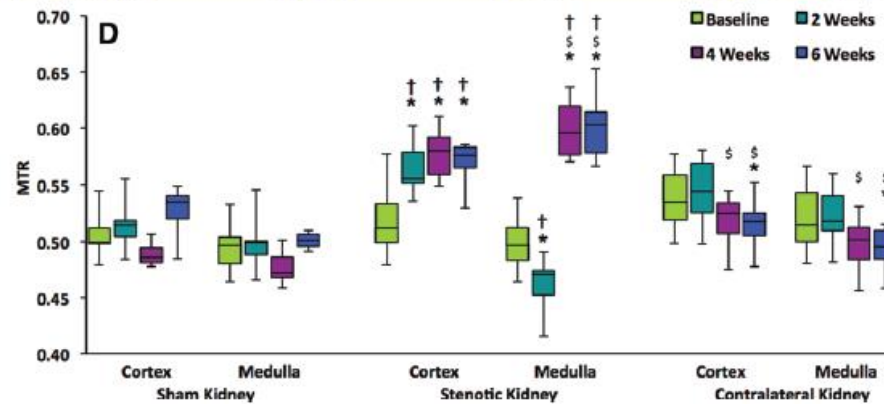
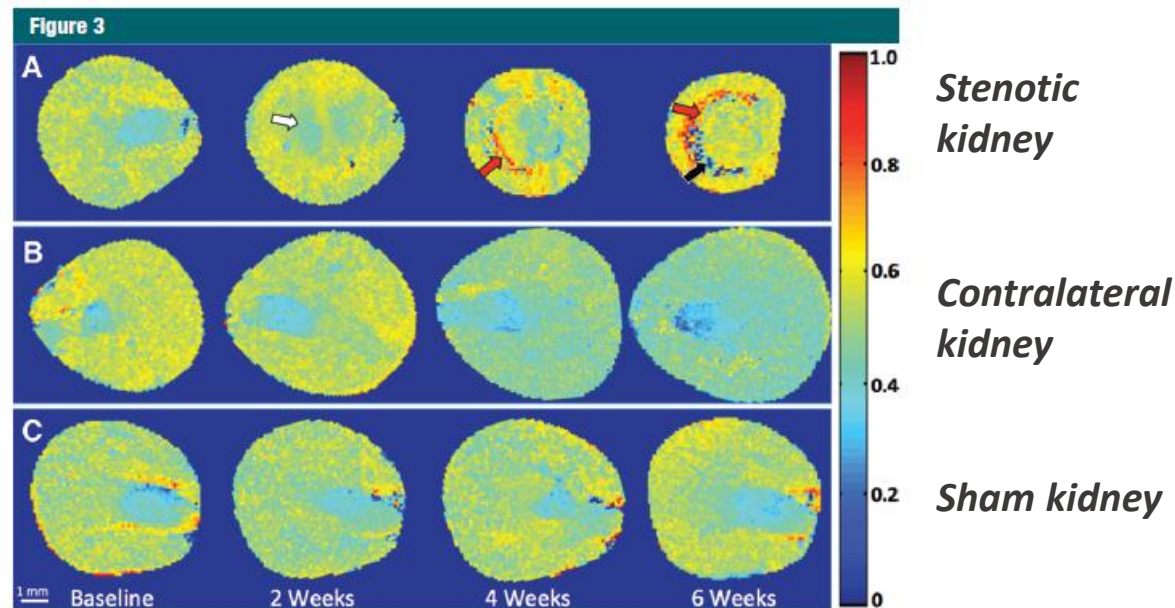
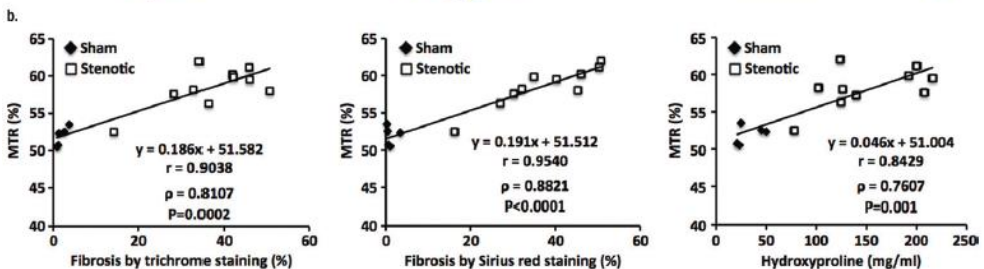
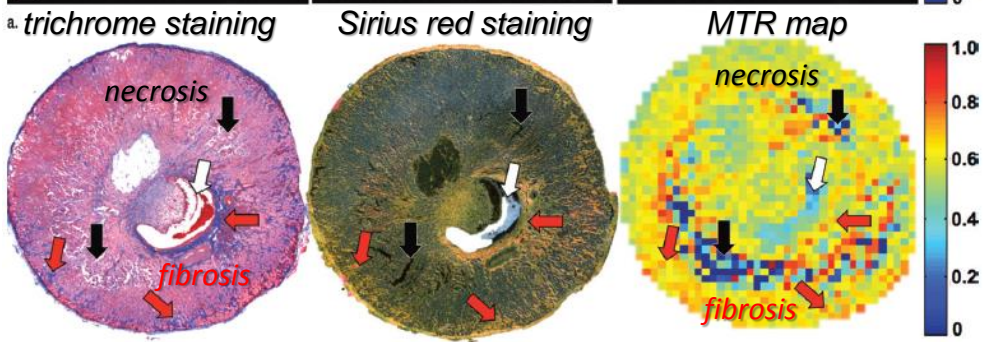
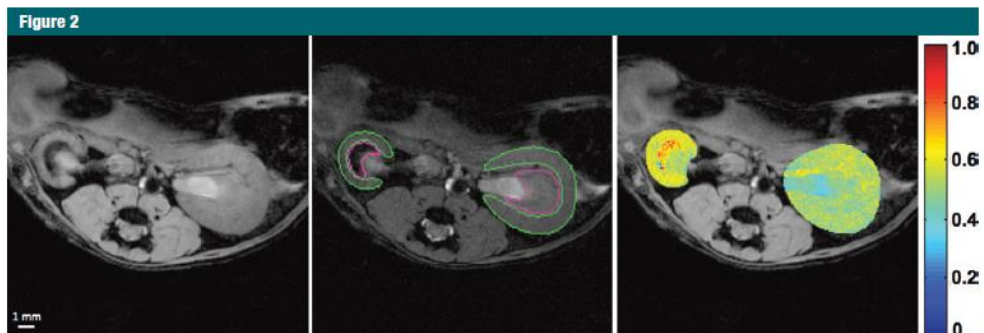
Kai Jiang, PhD
Christopher M. Ferguson, MS
Behzad Ebrahimi, PhD
Hui Tang, PhD
Timothy L. Kline, PhD
Tyson A. Burningham, BS
Prassana K. Mishra, PhD
Joseph P. Grande, MD, PhD
Slobodan I. Macura, PhD
Lilach O. Lerman, MD, PhD

Radiology: Volume 283: Number 1—April 2017

Noninvasive Assessment of Renal Fibrosis with Magnetization Transfer MR

Imaging: Validation and Evaluation in Murine Renal Artery Stenosis¹

- Renal artery stenosis (RAS) decreases renal blood flow (RBF) and causes a progressive loss of renal mass and function.
- Kidney undergoes a progressive deposition of extracellular matrix components (fibronectin and collagen type I, III, and IV) which may evolve into tubulointerstitial fibrosis.



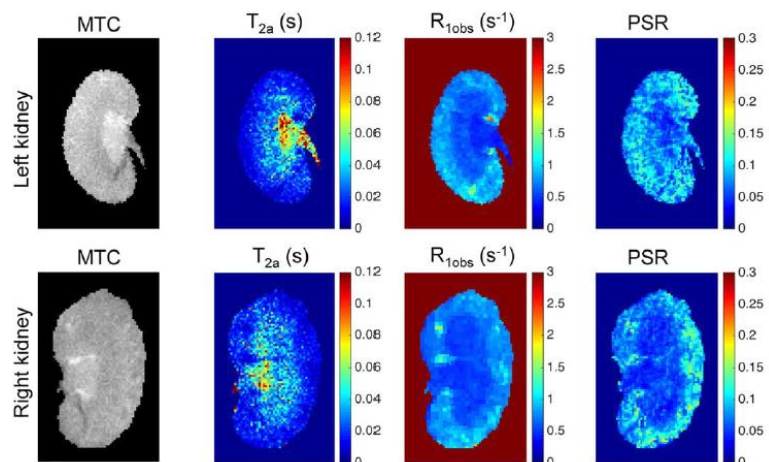
16.4T, RF @2.1 ppm, 10 μ Tx80ms

Assessment of renal fibrosis in murine diabetic nephropathy using quantitative magnetization transfer MRI

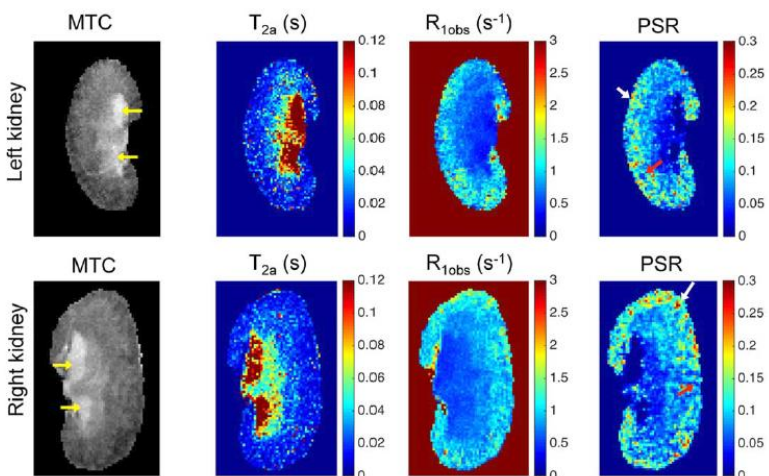
Feng Wang^{1,2*} | Daisuke Katagiri^{3*} | Ke Li¹ | Keiko Takahashi³ | Suwan Wang³ | Shinya Nagasaka^{3,4} | Hua Li^{1,2} | C. Chad Quarles^{1,2} | Ming-Zhi Zhang³ | Akira Shimizu⁴ | John C. Gore^{1,2} | Raymond C. Harris³ | Takamune Takahashi³

- Diabetic nephropathy (DN) is a major diabetic complication
- Renal fibrosis is a hallmark of progressive kidney disease, including DN
- db/db mice that lack the eNOS gene exhibit advanced DN similar to that found in human DN

Wild-type (9-week)



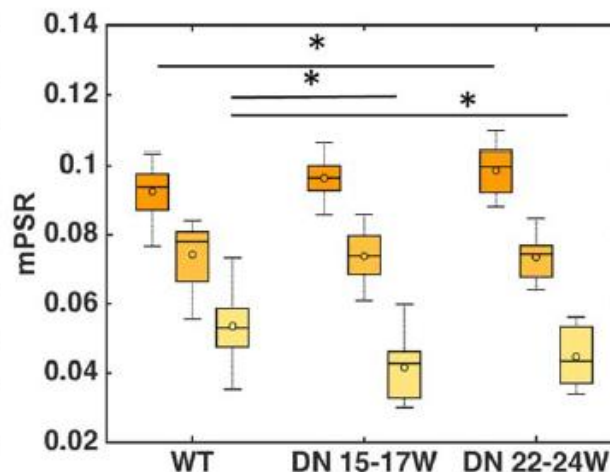
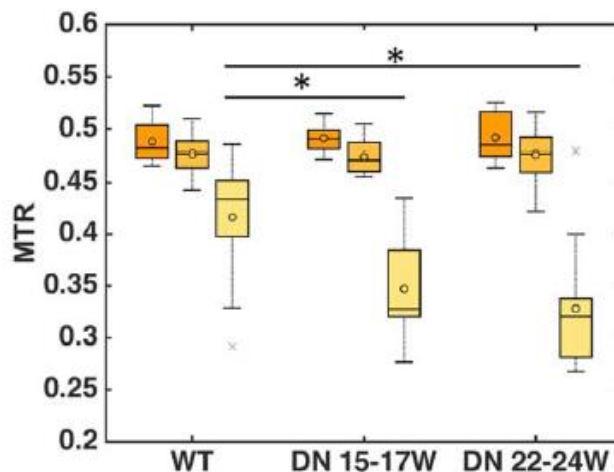
db/db -eNOS^{-/-} (24-week)



Henkelman-Ramani's model:

$$SI(\omega_1, \Delta f) = \frac{M_0 \left(R_b \left[\frac{RM_{0b}}{R_a} \right] + R_{RFB}(\omega_{1CWPE}, \Delta f, T_{2b}) + R_b + \frac{RM_{0b}}{F} \right)}{\left[\frac{RM_{0b}}{R_a} \right] \left(R_b + R_{RFB}(\omega_{1CWPE}, \Delta f, T_{2b}) \right) + \left(1 + \left[\frac{\omega_{1CWPE}}{2\pi\Delta f} \right]^2 \left[\frac{1}{T_{2a}R_a} \right] \right) \left(R_{RFB}(\omega_{1CWPE}, \Delta f, T_{2b}) + R_b + \frac{RM_{0b}}{F} \right)}$$

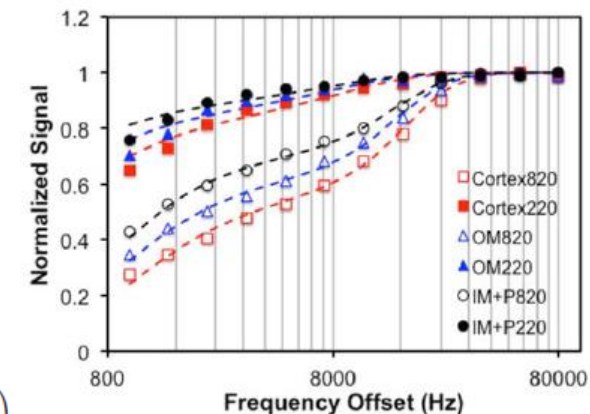
F = relative size of the macromolecular pool (PSR)



Cortex: increased fibrosis

OM, IM+P: urine retention

Cortex (dark orange)
OM (light orange)
IM+P (yellow)



7T, RF @3-266 ppm, 820°x20ms

Quantitative MRI of kidneys in renal disease

Timothy L. Kline¹, Marie E. Edwards², Ishan Garg¹, Maria V. Irazabal², Panagiotis Korfiatis¹, Peter C. Harris², Bernard F. King¹, Vicente E. Torres², Sudhakar K. Venkatesh¹, Bradley J. Erickson¹

test–retest reproducibility

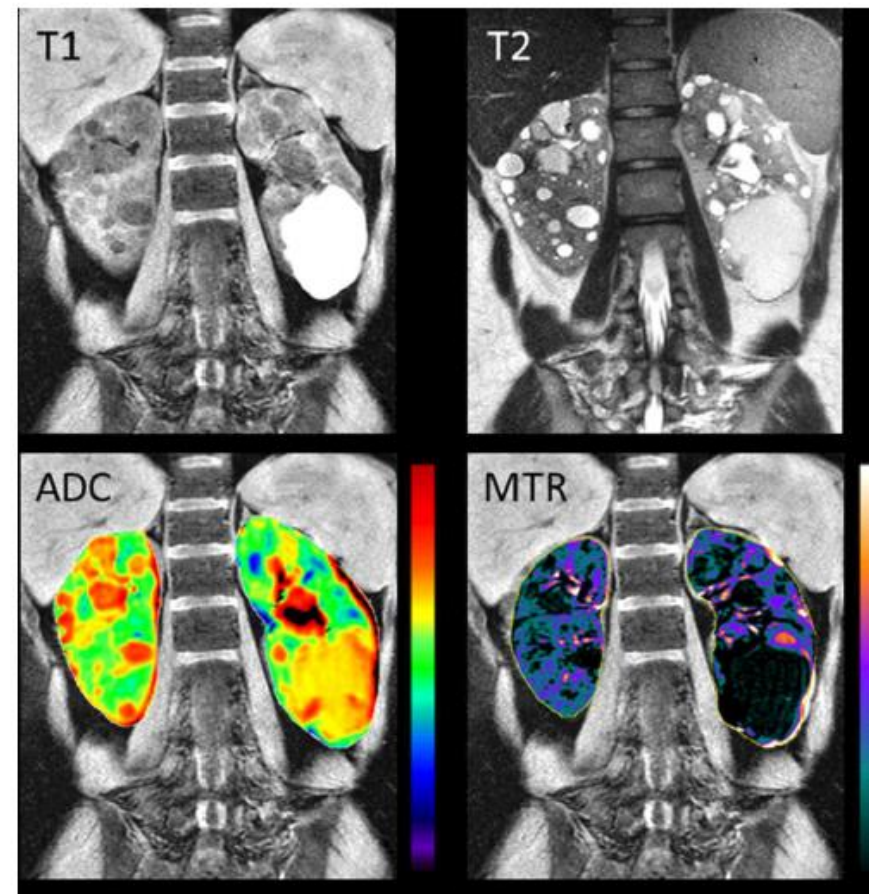
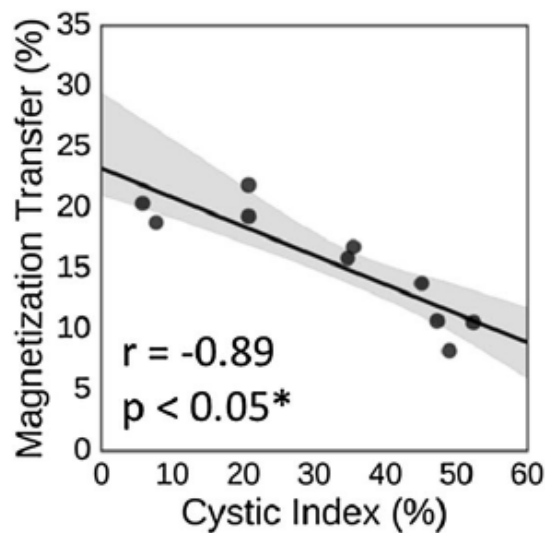
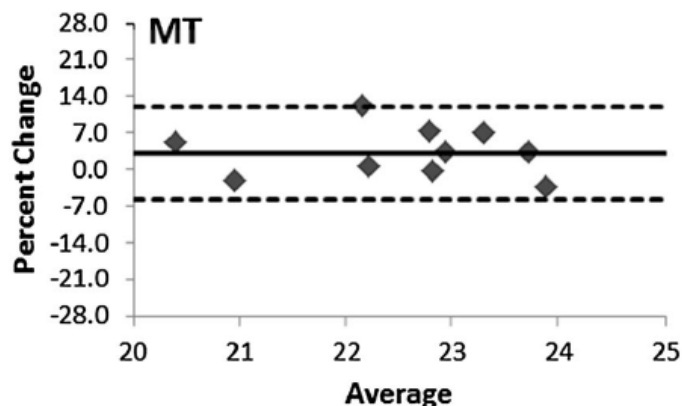


Table 3. Characteristics of the 20 patients in this study comparing the controls to the ADPKD patients for quantitative MR measurements

Scan	Parameter	Control	ADPKD	<i>p</i> value
BOLD	R2* (s ⁻¹)	18.1 ± 1.6	14.9 ± 1.7	0.002*
DWI	ADC (×10 ⁻³ mm ² /s)	2.18 ± 0.10	2.46 ± 0.20	0.013*
DWI	PF (%)	15.05 ± 3.97	12.48 ± 3.39	0.121
DWI	D (×10 ⁻³ mm ² /s)	2.08 ± 0.21	3.04 ± 1.86	0.005*
DWI	D* (×10 ⁻³ mm ² /s)	32.44 ± 17.25	27.65 ± 12.20	0.734
MT	MTR (%)	23.8 ± 1.2	16.3 ± 4.4	<0.001*
MRE	Tissue Stiffness (kPa)	3.8 ± 0.5	3.2 ± 0.3	0.016*

3T, RF @12 ppm

NCRP: non-cystic renal parenchyma patients (18-30 years old)

ADPKD: autosomal dominant polycystic kidney disease patients with normal renal function

CEST (CHEMICAL EXCHANGE SATURATION TRANSFER)

Journal of Magnetic Resonance **143**, 79–87 (2000)

A New Class of Contrast Agents for MRI Based on Proton Chemical Exchange Dependent Saturation Transfer (CEST)

K. M. Ward,¹ A. H. Aletras, and R. S. Balaban²

TABLE 1

Chemical-Exchange-Dependent Saturation Transfer Data from All Compounds Evaluated in this Study

Compound ^a	Conc (mM)	Functional group	ppm ^b	pH ^c	M_S/M_0	$M_0 - M_S$ (%)
Sugars^d						
<u>Hydroxyl protons (-OH)</u>						
Mannitol	250 mM	-OH	1.000	7.0	0.89	9.0
Sorbitol	250 mM	-OH	1.000	7.0	0.88	7.3
Fructose	250 mM	-OH	1.333	7.0	0.88	9.3
Dextrose	250 mM	-OH	1.500	7.0	0.89	8.7
Galactose	250 mM	-OH	1.167	7.0	0.85	10.3
Sucrose	250 mM	-OH	1.333	7.0	0.86	10.2
Maltose	250 mM	-OH	1.500	7.0	0.79	14.8
Lactose	250 mM	-OH	1.333	7.0	0.68	20.9
Dextran^e						
1.75 gm/100 ml	0.25 mM	-OH	1.167	7.0	0.91	8.1
3.50 gm/100 ml	0.5 mM	-OH	1.333	7.0	0.88	10.2
7.00 gm/100 ml	1.0 mM	-OH	1.333	7.0	0.81	13.6
14.0 gm/100 ml	2.0 mM	-OH	1.500	7.0	0.76	18.9
Amino acids^f						
<u>Amino protons (-NH₂)</u>						
L-Alanine	125 mM	-NH ₂	3.000	4.0	0.36	67.4
L-Arginine	125 mM	-NH ₂	3.000	4.0	0.36	65.8
<u>Guanidinium protons</u>						
L-Arginine	125 mM	Guanidinium protons	2.000	5.0	0.33	57.7
L-Lysine	125 mM	-NH ₂	3.000	4.0	0.34	66.2
L-Glutamine ^g	125 mM	-NH ₂	2.000	5.2	0.70	27.6
L-Tryptophan ^e	35 mM	-NH ₂	2.000	6.5	0.89	12.2
5-Hydroxytryptophan ^h	62.5 mM	-NH ₂	2.833	4.0	0.57	41.6

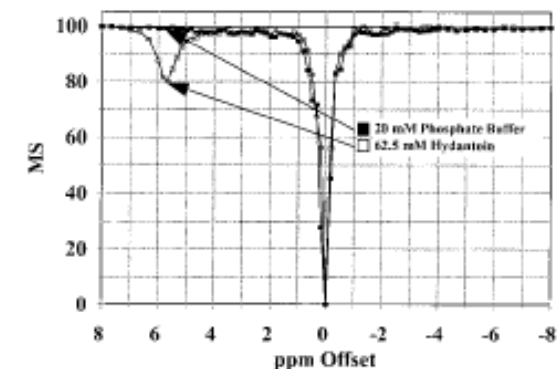
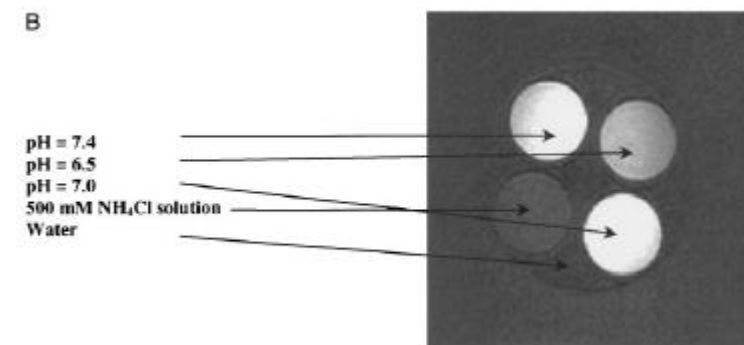


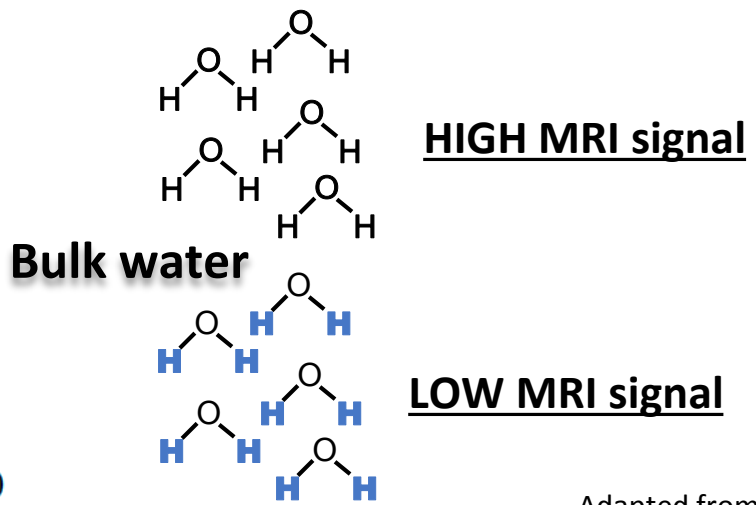
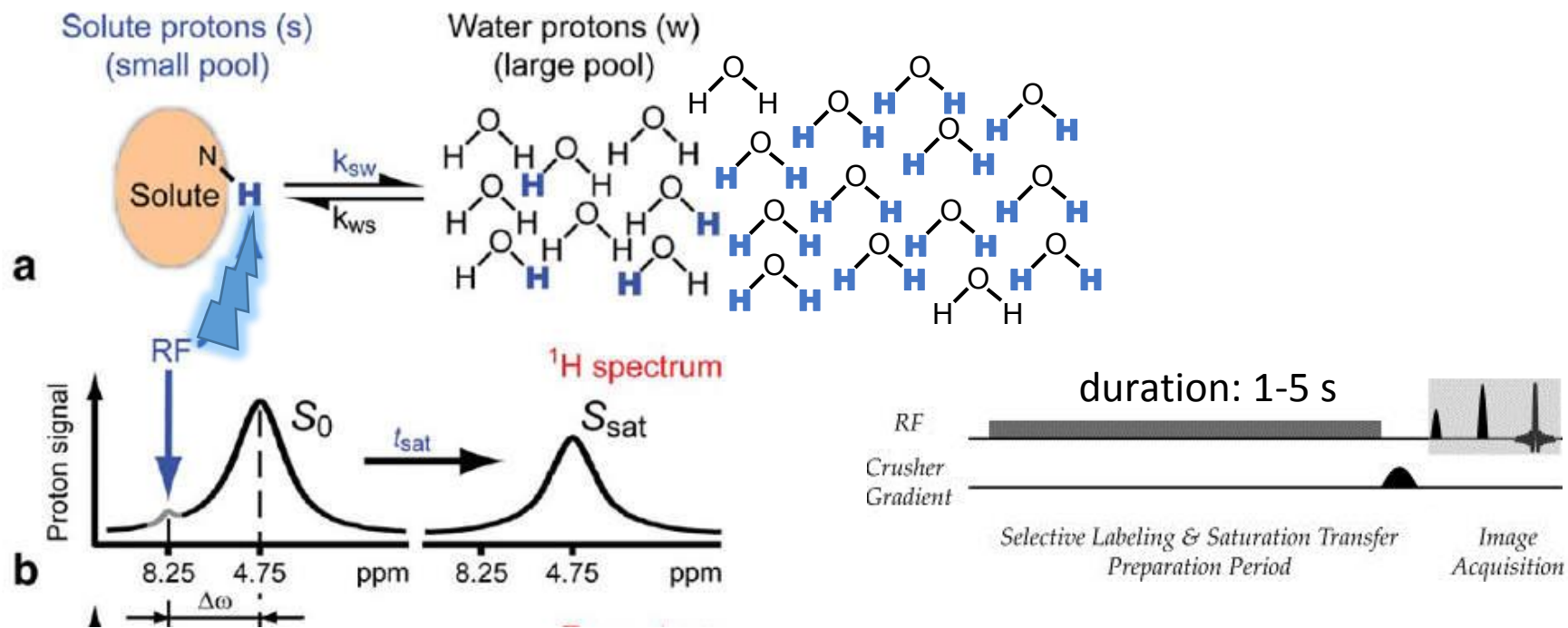
FIG. 1. Representative chemical exchange dependent saturation transfer (CEST) spectra of phosphate buffer (20 mM, pH 4.0) and hydantoin (62.5 mM, 20 mM phosphate buffer, pH 4.0) solutions at $T = 37^\circ\text{C}$.



CEST: HOW IT WORKS

NMR

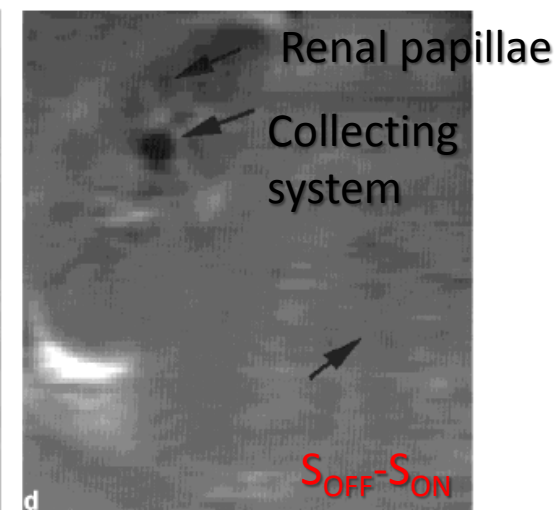
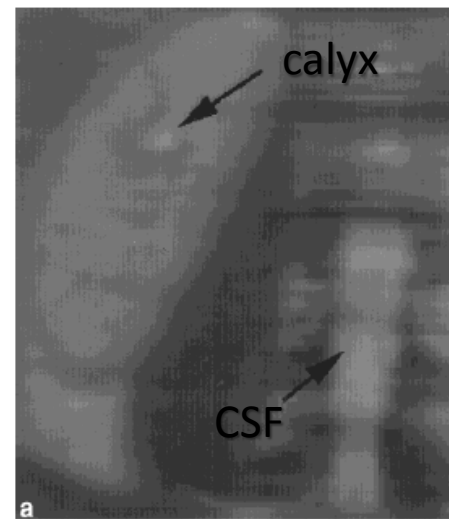
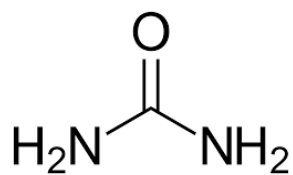
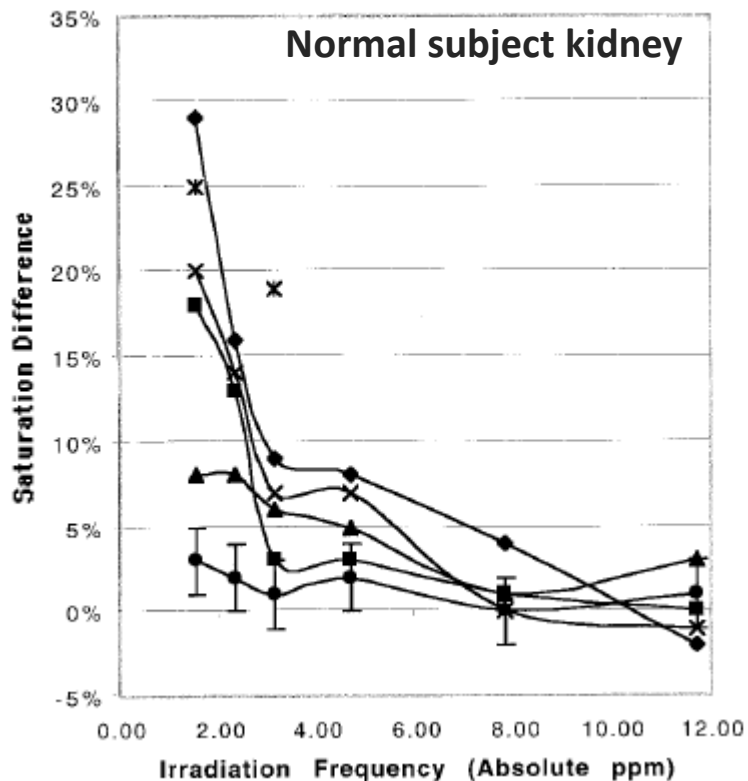
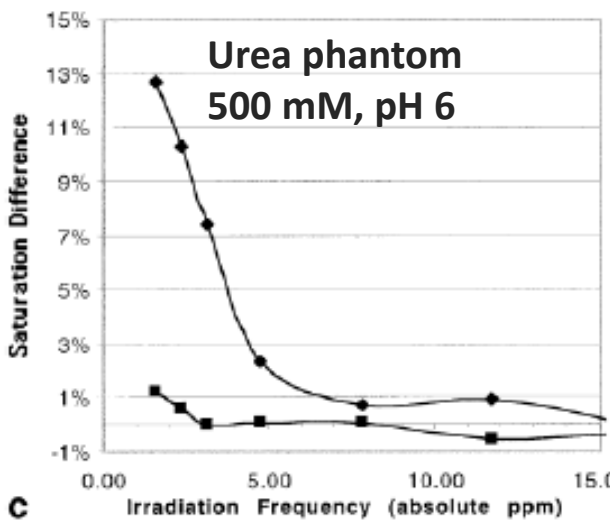
MRI



$$MTR_{asym}(\Delta\omega) = \{S_{sat}(-\Delta\omega) - S_{sat}(\Delta\omega)\} / S_0$$

Imaging of Urea Using Chemical Exchange-Dependent Saturation Transfer at 1.5 T

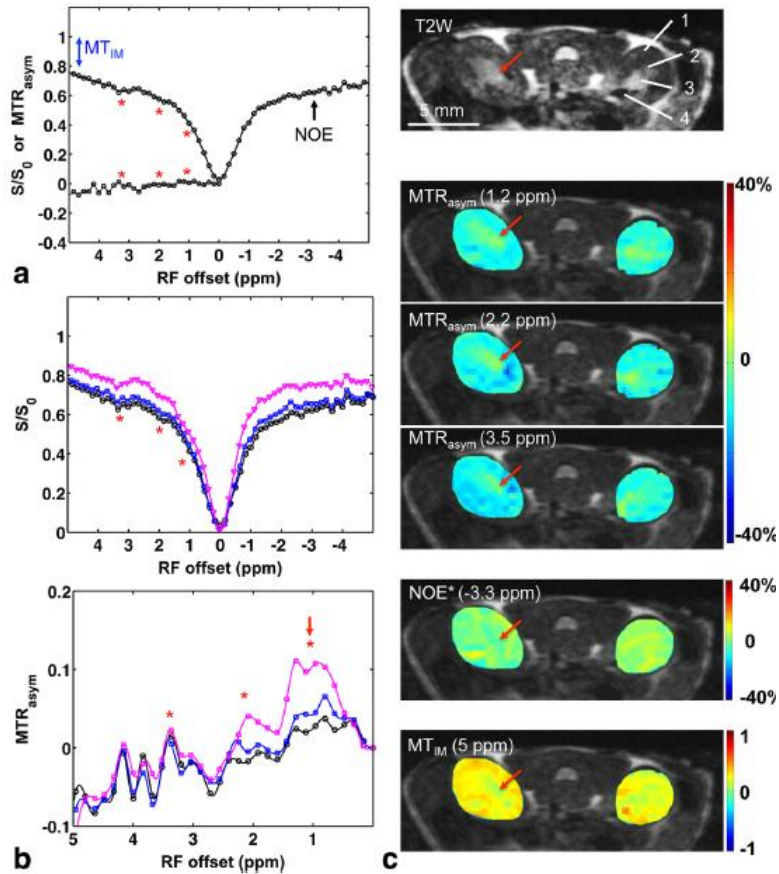
Azar P. Dagher, MD,* Anthony Aletras, PhD, Peter Choyke, MD, and Robert S. Balaban, PhD



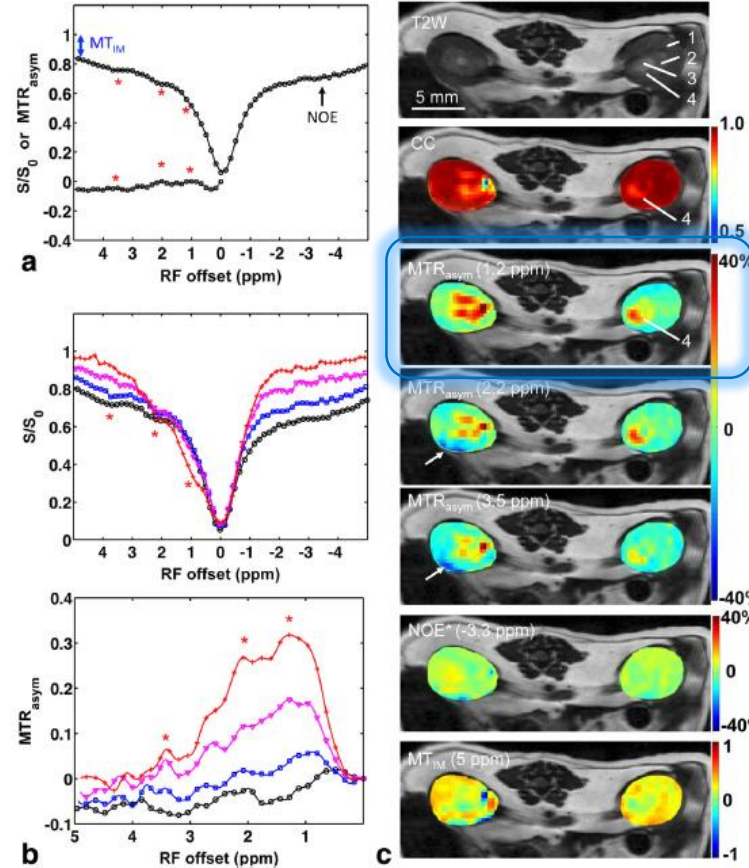
Mapping Murine Diabetic Kidney Disease Using Chemical Exchange Saturation Transfer MRI

Feng Wang,^{1,2*} David Kopylov,³ Zhongliang Zu,^{1,2} Keiko Takahashi,⁴ Suwan Wang,⁴ C. Chad Quarles,^{1,2} John C. Gore,^{1,2,5} Raymond C. Harris,⁴ and Takamune Takahashi⁴

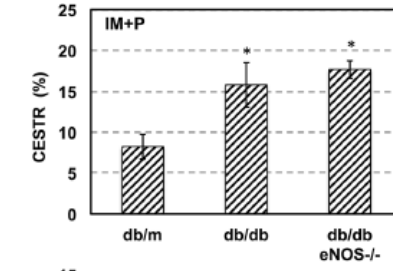
- Diabetic kidney disease is associated with changes in tissue metabolites (glucose, glycogen)
- Db/db mice (carry leptin receptor deficiency for type 2 diabetes) and db/db eNOS^{-/-} show advanced nephropathy



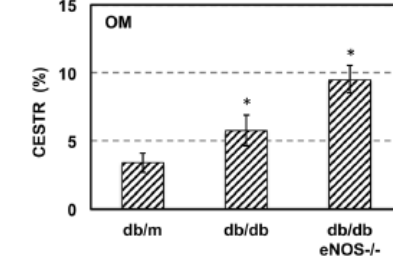
a Nondiabetic db/m mouse (16 weeks)



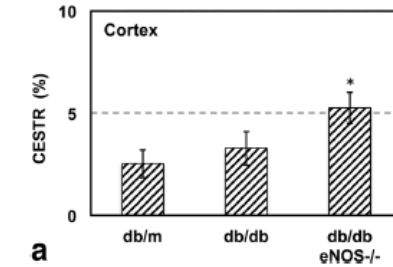
b diabetic db/db mouse (16 weeks)



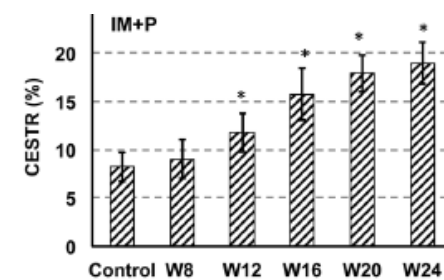
Increased glucose in urine



Increased glycogen deposition



Increased glucose uptake

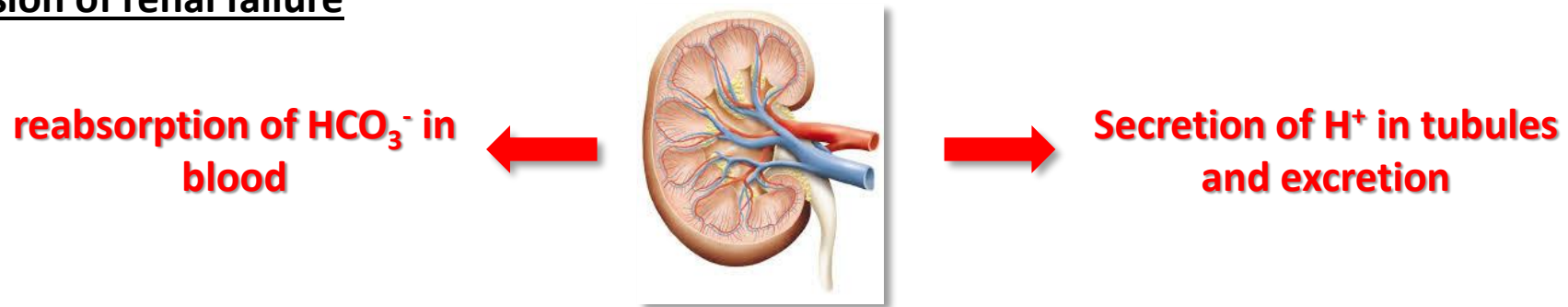


db/db mice

7T, RF @1.2 ppm, 1 μTx5s

KIDNEY REGULATION OF ACID-BASE HOMEOSTASIS

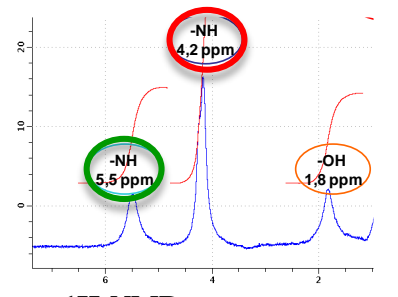
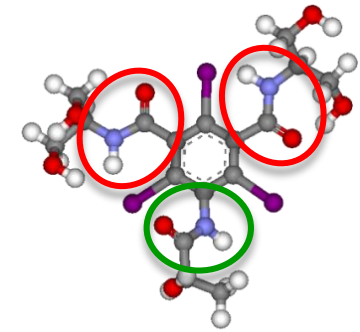
- ❑ The kidneys play a major role in the regulation of acid-base balance by reabsorbing bicarbonate filtered by the glomeruli and excreting titratable acids and ammonia into the urine
- ❑ Decline in kidney function will result in derangements in acid-base homeostasis with reduced ammonia excretion, inability to reabsorb bicarbonate and failure of acid excretion when kidney function is severely impaired
- ❑ In chronic kidney disease (CKD), with declining kidney function, acid retention and metabolic acidosis occur
- ❑ Degree of acidosis approximately correlates with severity of renal failure and usually is more severe at a lower GFR
- ❑ Several adverse consequences have been associated with metabolic acidosis, including muscle wasting, bone disease and progression of renal failure



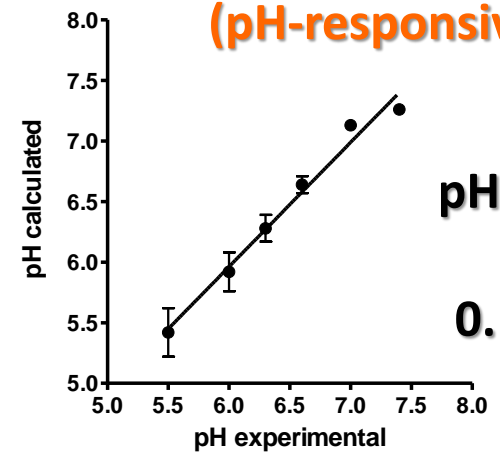
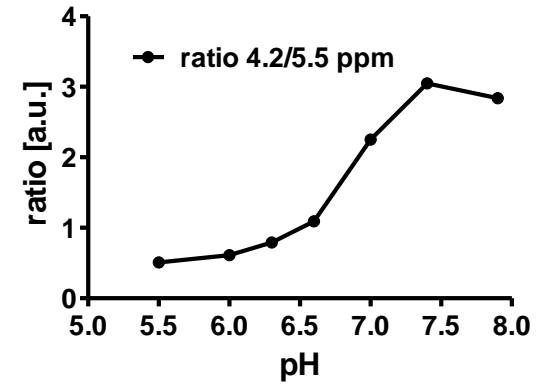
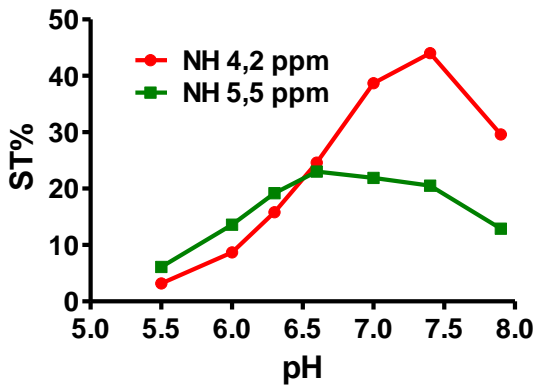
Renal pH mapping may represent a novel biomarker for detecting (early) renal damage

Iopamidol as a Responsive MRI-Chemical Exchange Saturation Transfer Contrast Agent for pH Mapping of Kidneys: In Vivo Studies in Mice at 7 T

Dario Livio Longo,¹ Walter Dastrù,¹ Giuseppe Digilio,² Jochen Keupp,³ Sander Langereis,³ Stefania Lanzardo,⁴ Simone Prestigio,⁴ Oliver Steinbach,³ Enzo Terreno,¹ Fulvio Uggeri,⁵ and Silvio Aime^{1*}

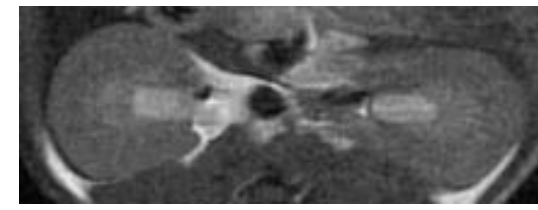


Iopamidol
(pH-responsive contrast agent)

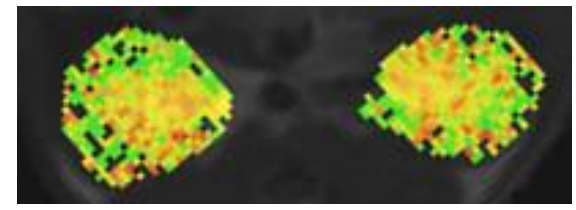


pH accuracy
 \approx
0.1 pH unit

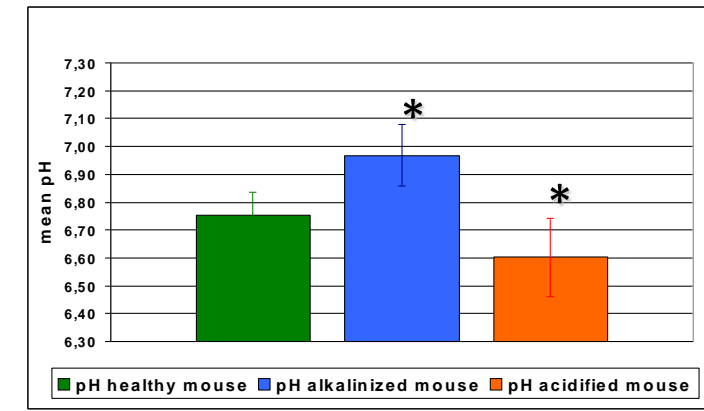
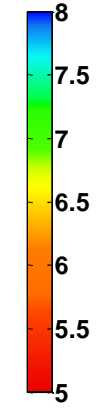
Ratiometric approach:
rule out the concentration term



T_{2w} anatomical image



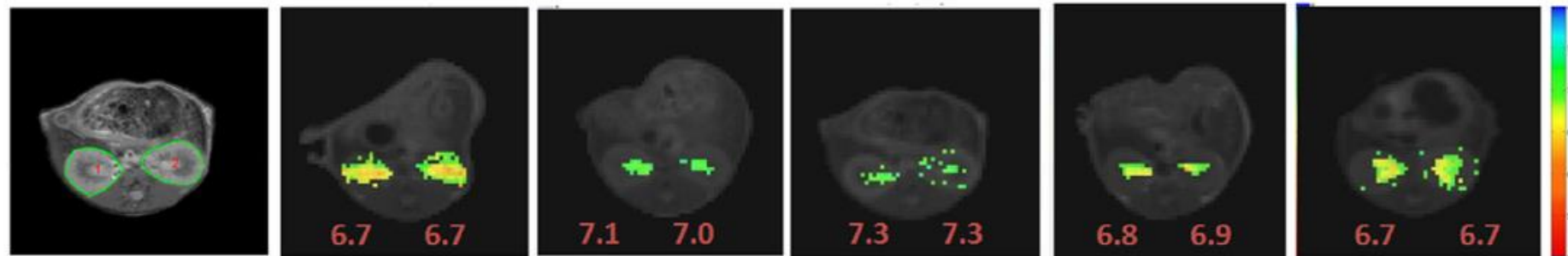
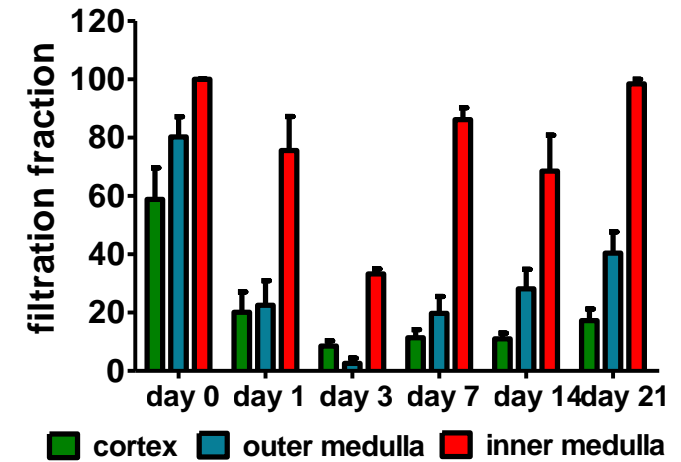
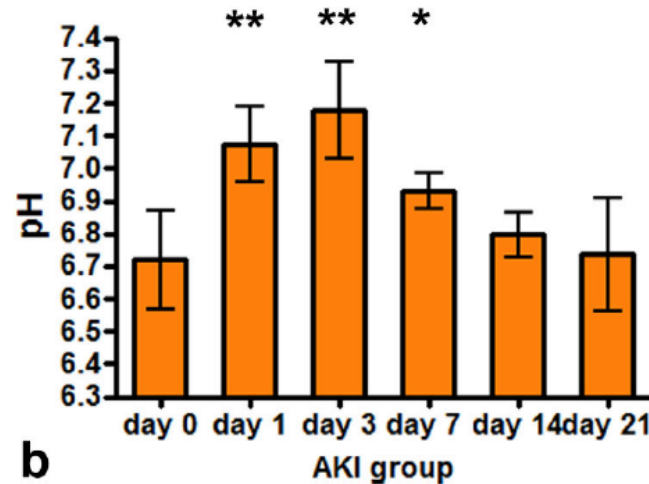
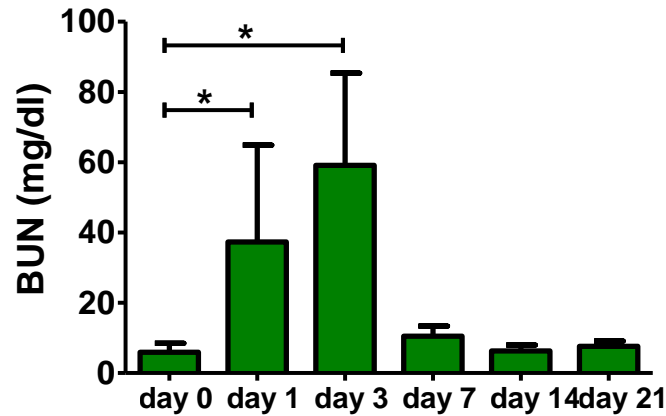
pH map



Imaging the pH Evolution of an Acute Kidney Injury Model by Means of Iopamidol, a MRI-CEST pH-Responsive Contrast Agent

Dario Livio Longo,¹ Alice Busato,¹ Stefania Lanzardo,² Federica Antico,³ and Silvio Aime^{1*}

- rhabdomyolysis is one of the leading causes of acute renal failure, initiated by acute disruption of skeletal muscle due to physical or chemical damage from crush injury, surgery, or toxins that may result in a rapid deterioration of renal function
- glycerol-induced AKI model show multiple ischemic, toxic, and obstructive tubular insults similar to acute tubular necrosis that occurs in humans



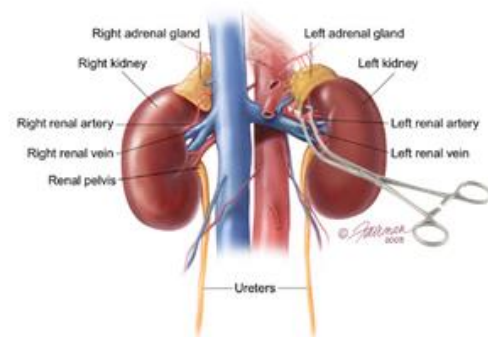
b T₂w Day 0 Day 1 Day 3 Day 7 Day 21

pH
Intramuscular injection
8 ml/kg (50% glycerol)

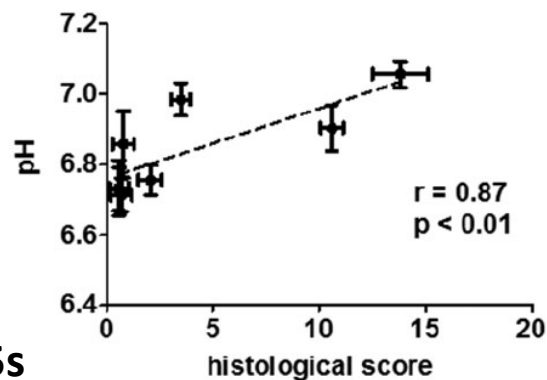
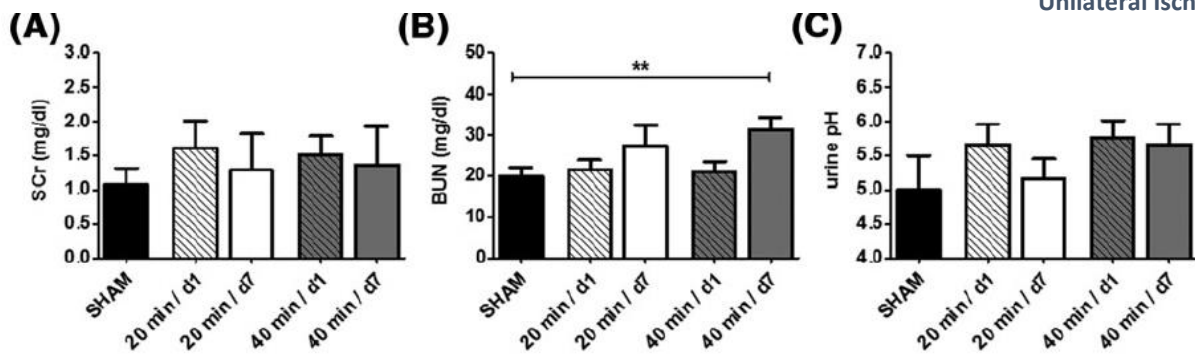
Noninvasive evaluation of renal pH homeostasis after ischemia reperfusion injury by CEST-MRI

Dario Livio Longo^{1,2} | Juan Carlos Cutrin² | Filippo Michelotti² | Pietro Irrera² | Silvio Aime²

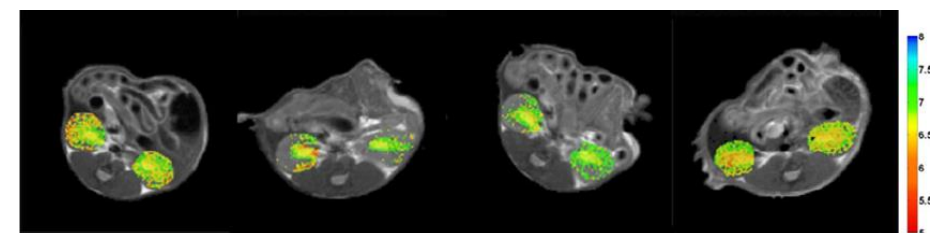
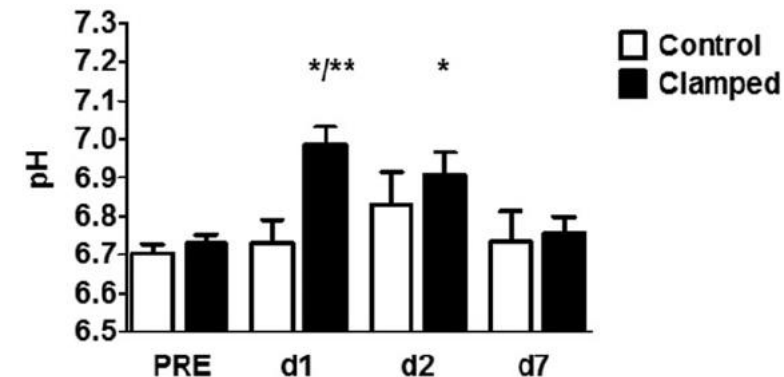
- Ischemic renal injury is the major cause of acute kidney injury (AKI)
- In the unilateral ischemia reperfusion injury (KIRI) model only one kidney is damaged and the contralateral compensate the reduced renal functionality



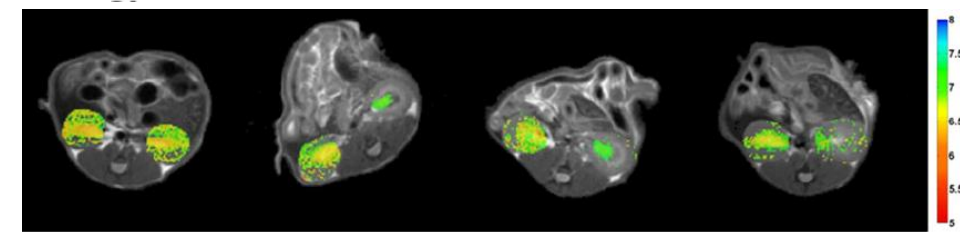
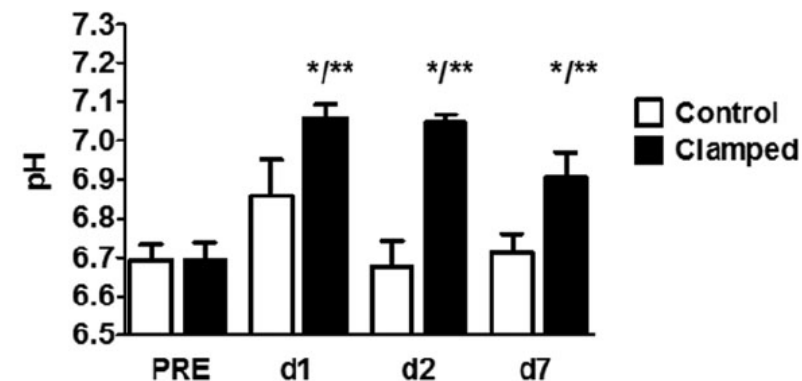
Unilateral Ischemic / Reperfusion Injury model



Moderate AKI (20 min ischemia)



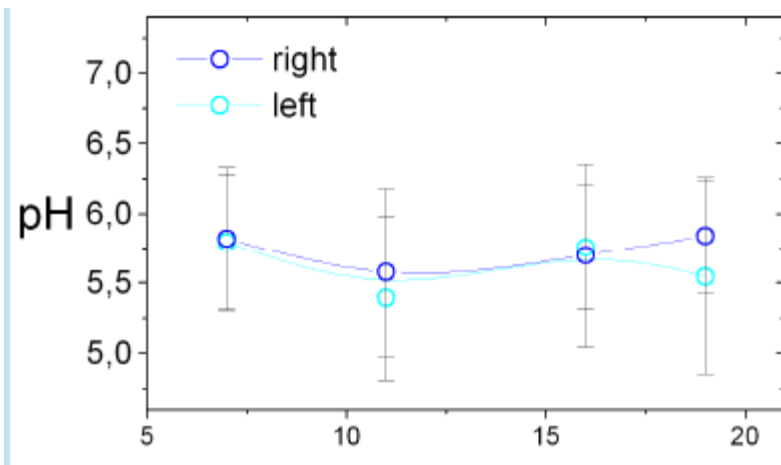
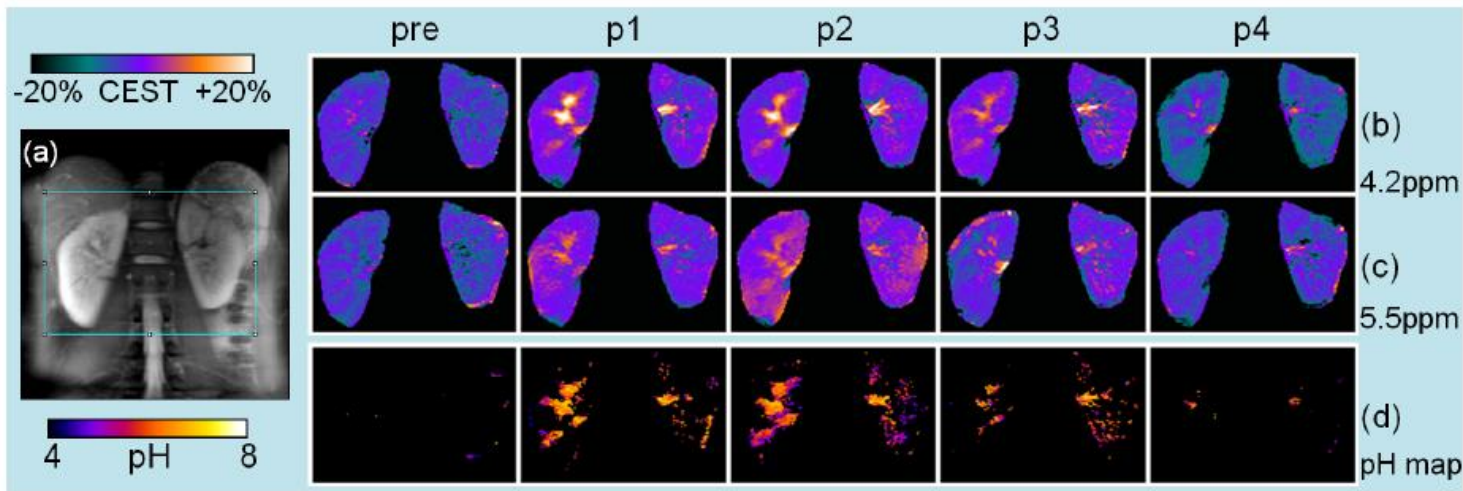
Severe AKI (40 min ischemia)



IN VIVO HUMAN KIDNEY PH MAPPING AT 3T USING TIME-INTERLEAVED PARALLEL RF TRANSMISSION CEST

Ivan E Dimitrov^{1,2}, Masaya Takahashi², Koji Sagiya², A. Dean Sherry^{2,3}, and Jochen Keupp⁴

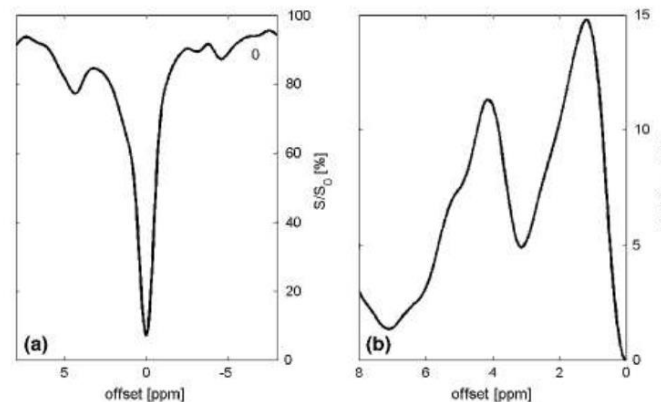
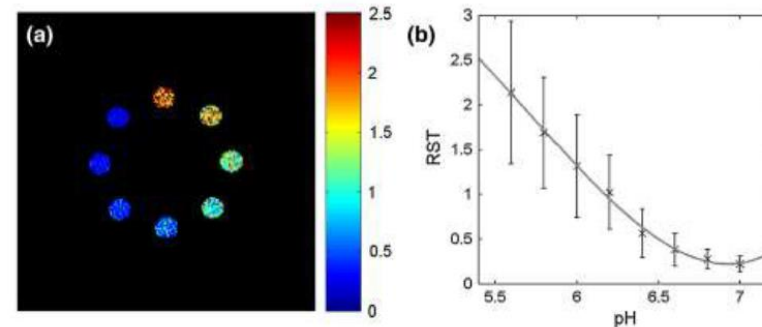
¹Philips Medical Systems, Cleveland, OH, United States, ²Advanced Imaging Research Center, University of Texas Southwestern Medical Center, Dallas, TX, United States, ³Chemistry, University of Texas Dallas, Richardson, TX, United States, ⁴Philips Research Europe, Hamburg, Germany



3T scanner (Achieva TX, Philips)
 RF 2.3 μ T, 2x49 ms
 100 ml iopamidol (Isovue 300), dose: 0.4 g I / kg

Pilot study of Iopamidol-based quantitative pH imaging on a clinical 3T MR scanner

Anja Müller-Lutz · Nadia Khalil · Benjamin Schmitt · Vladimir Jellus · Gael Pentang · Georg Oeltzschner · Gerald Antoch · Rotem S. Lanzman · Hans-Jörg Wittsack



**Human bladder
 CEST pH= 6.65
 Urine pH = 6.72**

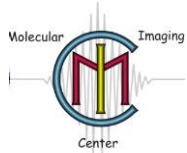
3T scanner (Magnetom Trio A, Siemens)
 RF 0.4 μ T, 10x100 ms
 65 min after CT examination



Italian National Research Council



UNIVERSITA' DEGLI STUDI DI TORINO



**University of Torino /
Molecular Imaging Center**

Silvio Aime
Enzo Terreno
Simonetta Geninatti
Eliana Gianolio
Daniela Delli Castelli
Walter Dastrù
Francesca Reineri
Juan Carlos Cutrin
Rachele Stefania
Francesca Arena
Enza Di Gregorio
Giuseppe Ferrauto
Eleonora Cavallari



**Institute of Biostructures
and Bioimaging / CNR**

Marcello Mancini
Giuseppina De Simone
Valeria Menchise
Sergio Padovan



University College London

Xavier Golay
Mina Kin
Eleni Demetriou
Aaron Kujawa



Moffitt Cancer Center

Robert Gillies
Pedro Enriquez-Navas
Damgaci Sultan



**Max Planck Institute
Tuebingen**

Moritz Zaiss, Rolf Pohmann



**Technische Universität München
Technische Universität
München**

Markus Schwaiger



**University of Eastern
Piedmont**

Mauro Botta
Giuseppe Digilio
Lorenzo Tei

MGH/HST Athinoula A. Martinos
Center for Biomedical Imaging



**A. Martinos Center
for Biomedical Imaging**
Christian Farrar
Or Perlman



מכון ויצמן למדע
WEIZMANN INSTITUTE OF SCIENCE

Weizmann Institute
Michal Neeman
Gadi Cohen



Emory University
Phillip Zhe Sun



LIFE FROM INSIDE

Bracco Imaging Spa

Fulvio Uggeri
Alessandro Maiocchi
Fabio Tedoldi
Sonia Colombo Serra



Aspect Imaging

Uri Rapoport
Peter Bendel
Michael Glekel
Yael Schifffenbauer



Istituto Ortopedico Rizzoli

Sofia Avnet
Nicola Baldini



University of Copenhagen
Stine Falsig Pedersen



Medical Faculty Mannheim
Frank Gerrit Zöllner

National grants:



EU projects:







Italian National
Research Council



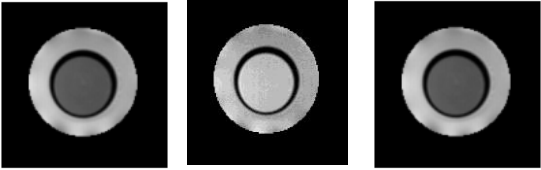
ADVANTAGES OVER CONVENTIONAL MRI CONTRAST AGENTS

CONTRAST

ALWAYS ON



SWITCHED ON/OFF AT WILL

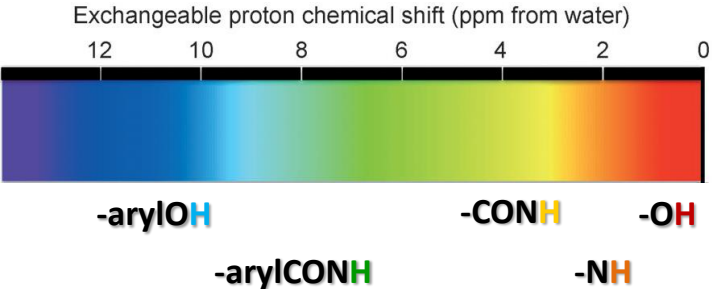


ON OFF ON

RELAXIVITY-ENCODED



FREQUENCY-ENCODED



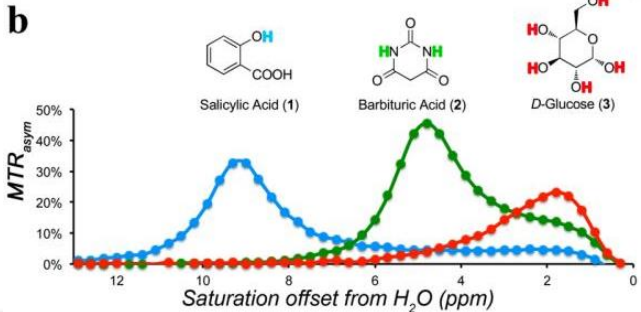
SINGLE VISUALIZATION



2*Gd1 or Gd1+Gd2

Gd1 or Gd2

MULTIPLE VISUALIZATION



GADOLINIUM-based

CEST-based

DISADVANTAGES TO CONVENTIONAL MRI CONTRAST AGENTS

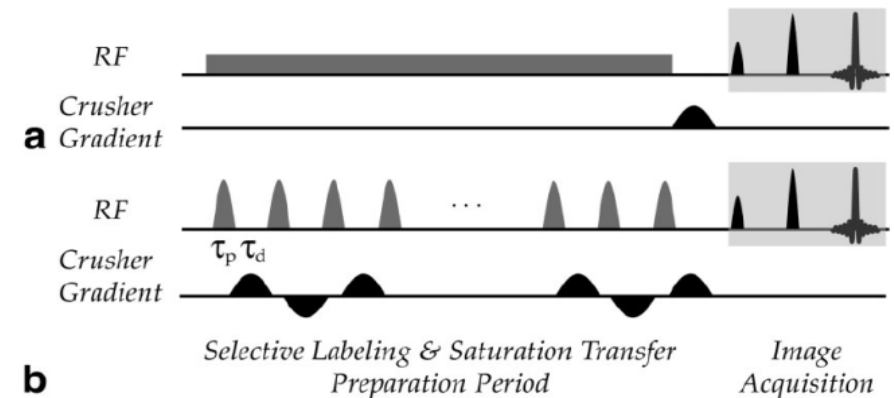
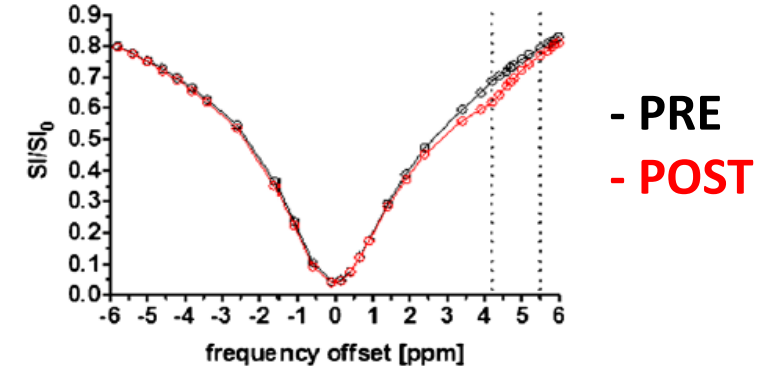
Specificity only for exogenous contrast agent

Low sensitivity (mM- μ M range, dependent on exchange rate / chemical shift / number of protons)

High magnetic field (≥ 3 T)

low temporal resolution (saturation module + multiple offsets)

SAR limitations (low/high B_1 , long/short period)



PRE-CLINICAL APPLICATIONS OF MRI-CEST pH-sensitive agents

PRECLINICAL AND CLINICAL IMAGING - Note

Magnetic Resonance in Medicine 70:859-864 (2013)

Imaging the pH Evolution of an Acute Kidney Injury Model by Means of Iopamidol, a MRI-CEST pH-Responsive Contrast Agent

Dario Livio Longo,¹ Alice Busato,¹ Stefania Lanzardo,² Federica Antico,³ and Silvio Aime^{1*}

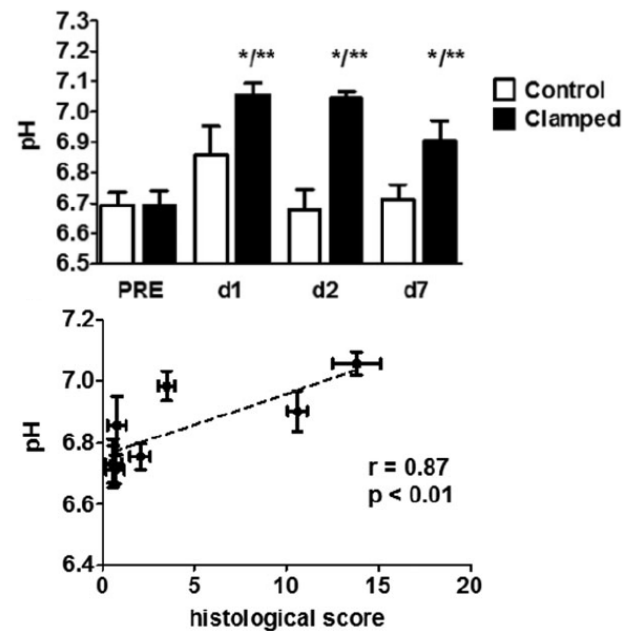
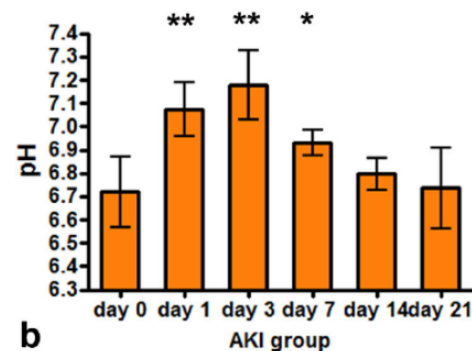
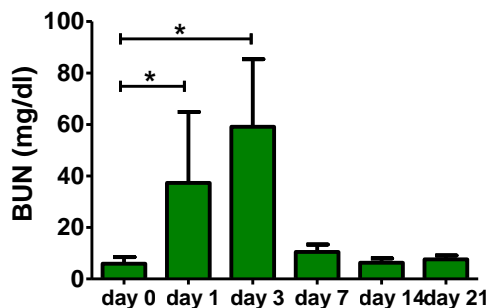
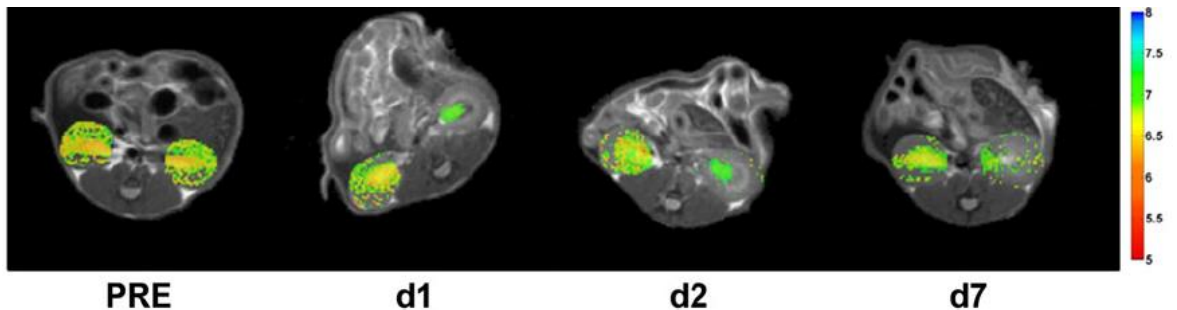
DOI 10.1002/nbm.3720

RESEARCH ARTICLE

WILEY **NMR** IN BIOMEDICINE

Noninvasive evaluation of renal pH homeostasis after ischemia reperfusion injury by CEST-MRI

Dario Livio Longo^{1,2} | Juan Carlos Cutrin² | Filippo Michelotti² | Pietro Irrera² | Silvio Aime²

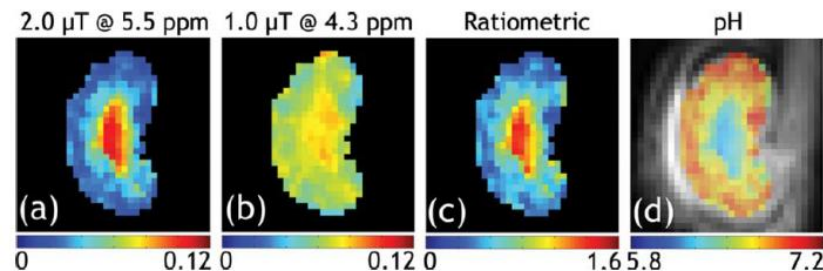


NOTE

Magnetic Resonance in Medicine 00:00-00 (2017)

A Generalized Ratiometric Chemical Exchange Saturation Transfer (CEST) MRI Approach for Mapping Renal pH using Iopamidol

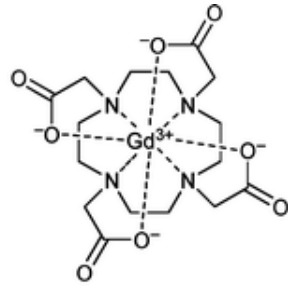
Yin Wu,^{1,2} Iris Y. Zhou,¹ Takahiro Igarashi,¹ Dario L. Longo,³ Silvio Aime,⁴ and Phillip Zhe Sun^{1*}



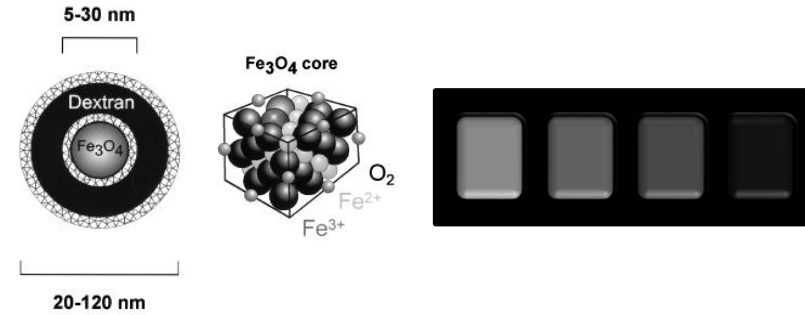
4.7 T, rats

CEST (CHEMICAL EXCHANGE SATURATION TRANSFER)

Gd-complexes and iron-oxide particles generate a relaxivity-based contrast



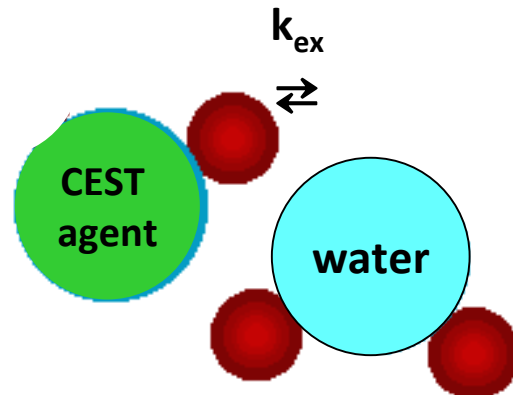
Gd-based / T₁ agents



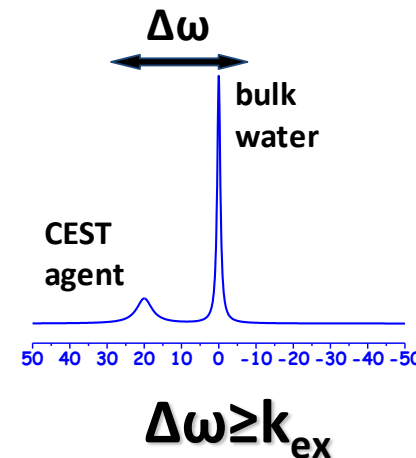
Iron oxide nanoparticles / T₂ agents

CEST agents generate a "frequency-encoded" MR contrast

mobile protons in exchange
with water molecules



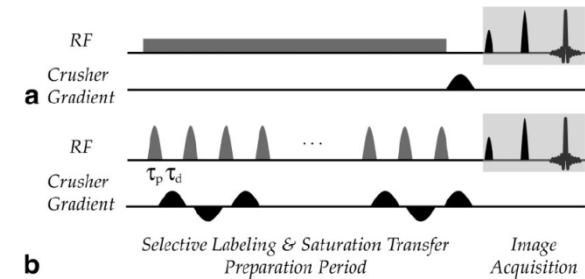
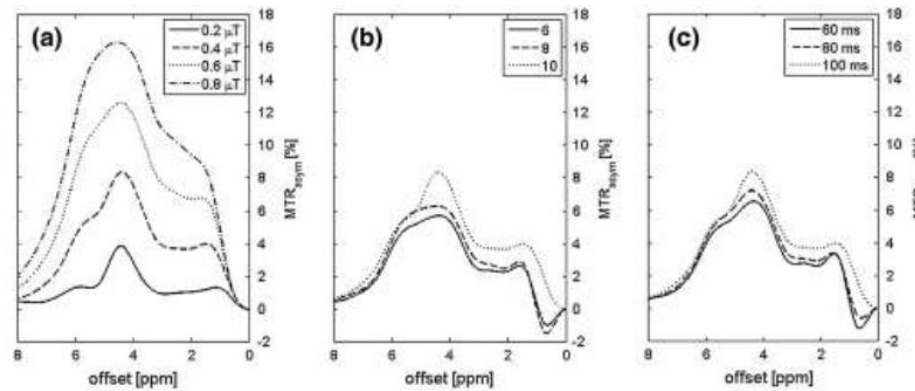
distinct NMR signals



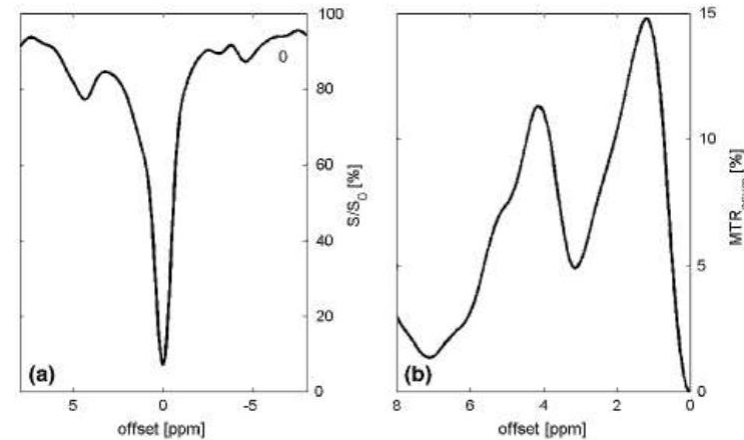
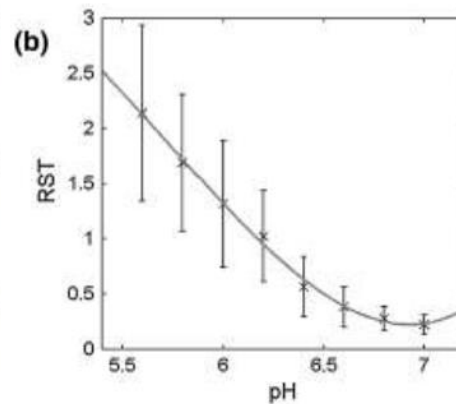
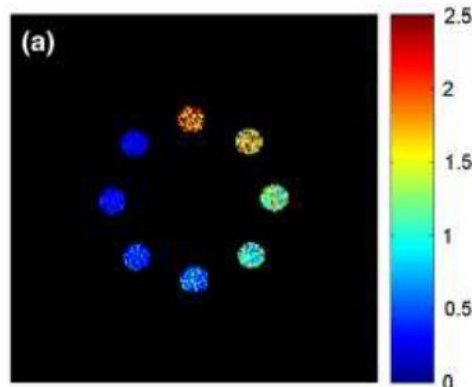
Pilot study of Iopamidol-based quantitative pH imaging on a clinical 3T MR scanner

Anja Müller-Lutz · Nadia Khalil · Benjamin Schmitt · Vladimir Jellus · Gael Pentang · Georg Oeltzschner · Gerald Antoch · Rotem S. Lanzman · Hans-Jörg Wittsack

Fig. 1 MTR_{asym} curves of the Iopamidol solution measured with different B_1 -CWAE field strengths (a), different number of pulses (b), and different pulse durations (c)

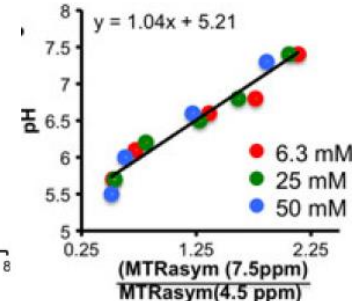
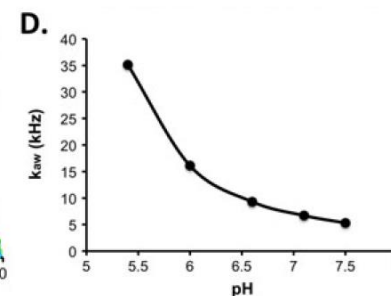
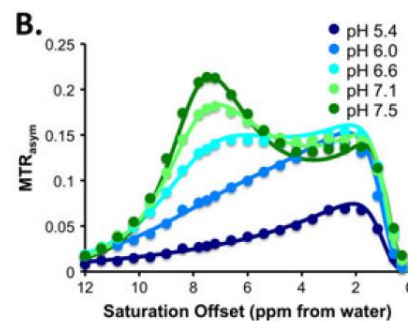
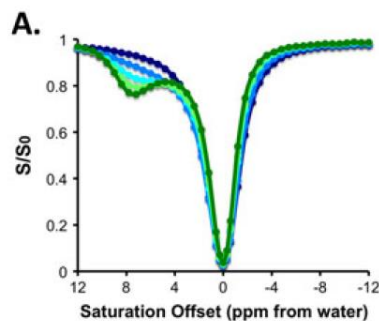
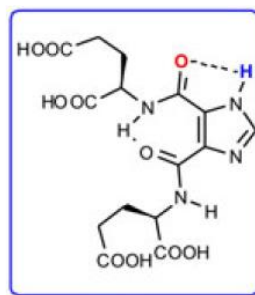


Human bladder
Iopamidol-CEST pH= 6.65
Urine pH = 6.72



Developing imidazoles as CEST MRI pH sensors

Xing Yang^{a†}, Xiaolei Song^{a,b†}, Sangeeta Ray Banerjee^a, Yuguo Li^{a,b}, Youngjoo Byun^c, Guanshu Liu^{a,b}, Zaver M. Bhujwala^a, Martin G. Pomper^{a*} and Michael T. McMahon^{a,b*}



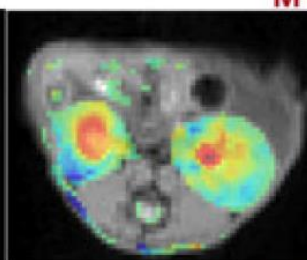
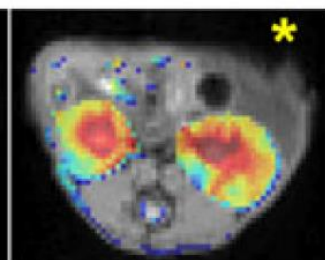
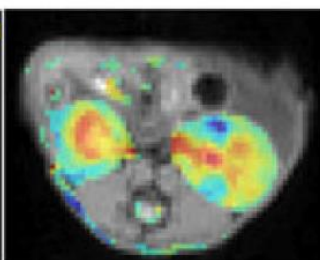
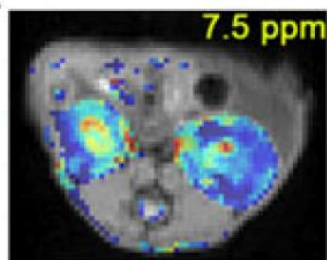
Pre-inject

Post- 35 min

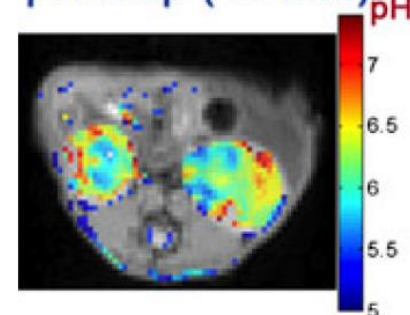
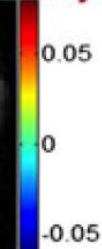
Post- 45 min

Post- 55 min

pH map (45 min)



MTRasym

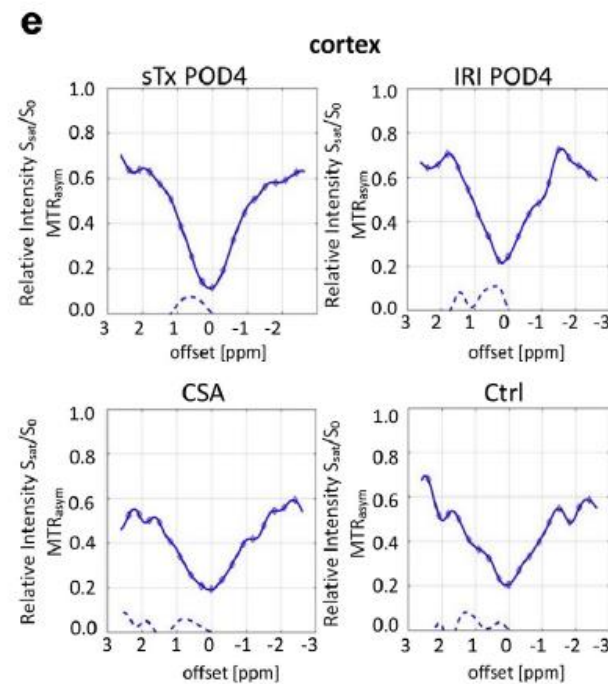
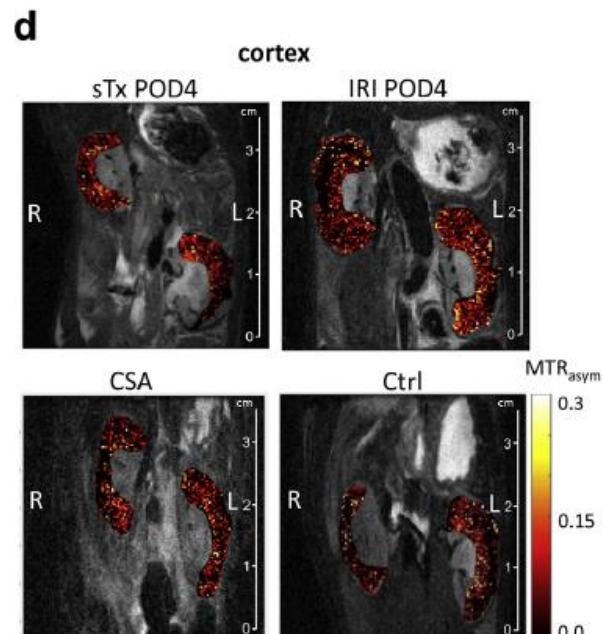
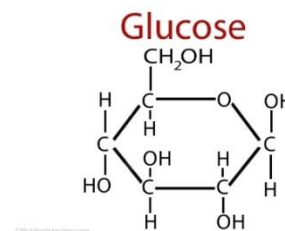


GlucoCEST magnetic resonance imaging *in vivo* may be diagnostic of acute renal allograft rejection

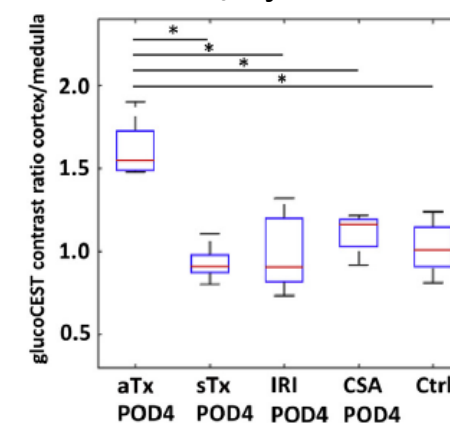


9.4 T

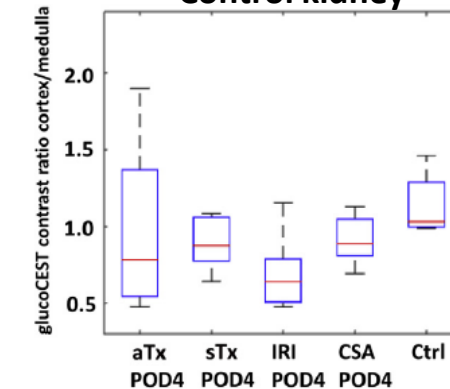
Dominik Kentrup^{1,8}, Philipp Bovenkamp^{2,8}, Annika Busch², Katharina Schuette-Nuetgen¹, Helga Pawelski¹, Hermann Pavenstädt¹, Eberhard Schlatter¹, Karl-Heinz Herrmann³, Jürgen R. Reichenbach³, Bettina Löffler⁴, Barbara Heitplatz⁵, Veerle Van Marck⁵, Nirbhay N. Yadav^{6,7}, Guanshu Liu^{6,7}, Peter C.M. van Zijl^{6,7}, Stefan Reuter^{1,9} and Verena Hoerr^{2,4,9}



a Grafted/injured kidney



b Control kidney



Imaging Agents

International Edition: DOI: 10.1002/anie.201502497
German Edition: DOI: 10.1002/ange.201502497

A pH-Responsive MRI Agent that Can Be Activated Beyond the Tissue Magnetization Transfer Window**

Xiaojing Wang, Yunkou Wu, Todd C. Soesbe, Jing Yu, Piyu Zhao, Garry E. Kiefer, and A. Dean Sherry*

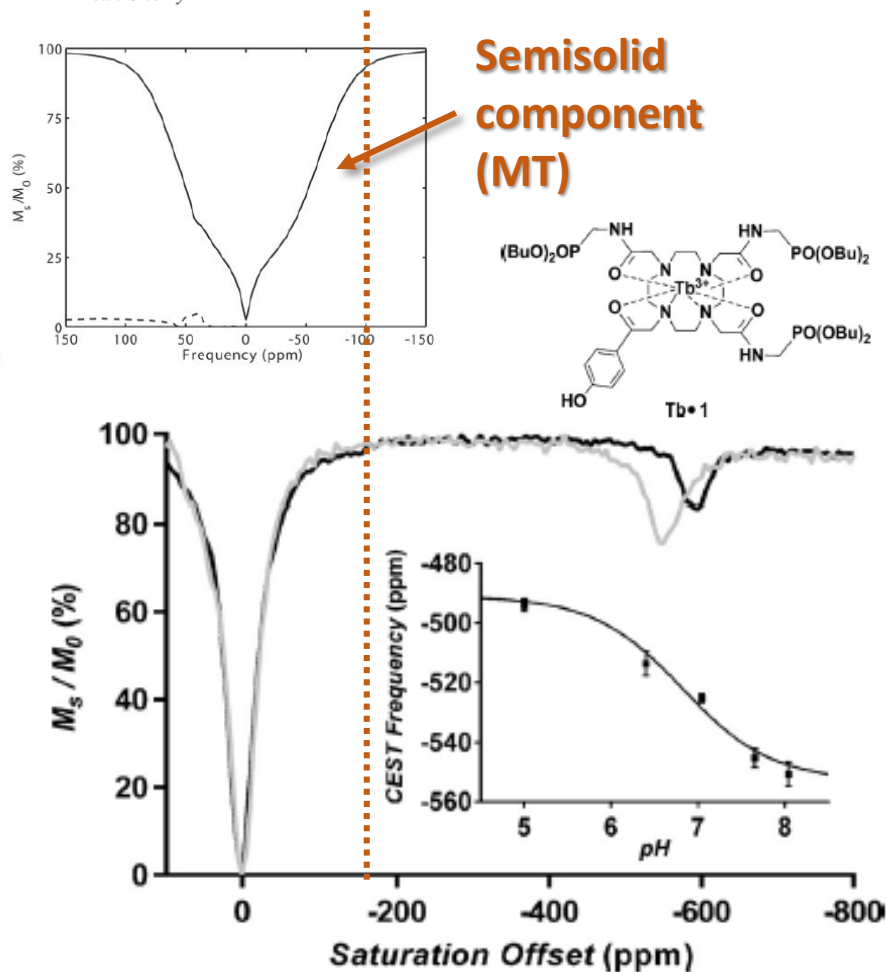


Figure 1. CEST spectra of 20 mM Tb-1 agent recorded at pH 8.2 at 298 K (black line) and 310 K (gray line) in CD₃CN/H₂O (1:1) with a B₁ of 100 μT. The inset shows a plot of the chemical shift of the water exchange CEST peak as a function of pH (T = 310 K).

pH Imaging of Mouse Kidneys In Vivo Using a Frequency-Dependent paraCEST Agent

Yunkou Wu,^{1,2,3} Shanrong Zhang,¹ Todd C. Soesbe,^{1,2} Jing Yu,⁴ Elena Vinogradov,^{1,2} Robert E. Lenkinski,^{1,2} and A. Dean Sherry^{1,2,4*}

